

More Inflation Tilings

DIRK FRETTLÖH

Inflation tilings exhibit a wealth of properties, as we shall demonstrate by means of explicit examples. In this sense, this chapter can be seen as an extension of [AO1, Ch. 6]. Along the journey, the concept of inflation will be generalised in several ways. One of the aims of our exposition is to highlight some of the more exotic behaviour that can be observed in the realm of inflation tilings and to point out some interesting questions raised by these examples. Most of the examples discussed below are contained in the Tilings Encyclopedia [21].

1.1. A simple inflation tiling without FLC

Many if not most examples of aperiodic tilings in the literature have *finite local complexity* (FLC); see [11] or [AO1, Sec. 5.3] for background. Even though these examples may be easier to construct, there is no reason to assume that FLC is a typical property of inflation tilings. One of the simplest inflation tilings that fails to have FLC is generated by the following rule [33]:

$$(1.1.1) \quad \begin{array}{c} 1 \\ \square \\ 1 \end{array} \longrightarrow \begin{array}{ccc} \square & \square & \square \\ \square & \square & \square \\ \square & \square & \square \end{array} \begin{array}{c} \updownarrow a \end{array}$$

The inflation factor (or multiplier) for this rule is 3, and the single prototile is a unit square. Under the inflation, each square is replaced by three columns of three squares each, where the third column is shifted vertically by some irrational number $a \notin \mathbb{Q}$. The resulting tilings contain pairs of squares sharing an entire edge, as well as pairs of squares sharing part of an edge, where vertical shifts of the form $na \bmod 1$ between adjacent squares are realised with infinitely many different $n \in \mathbb{N}$. In particular, the integer n takes the

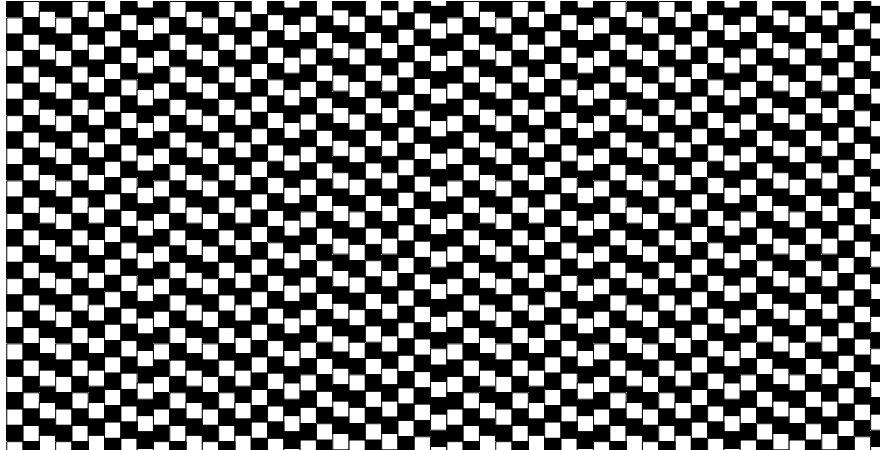
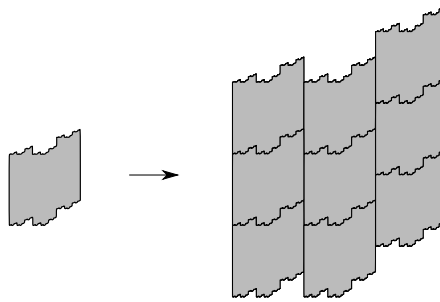


FIGURE 1.1.1. A patch of a simple non-FLC tiling, as defined by Eq. (1.1.1). For clarity, the square tiles are alternately coloured black and white.

values $1, 3+1, 3^2+3+1$ etc. Since a is irrational, the corresponding values of $na \bmod 1$ are all different. Consequently, there are infinitely many pairwise non-congruent clusters (or patches) of two adjacent tiles. This shows that the tilings obtained from this inflation rule do not have the FLC property. A patch of such a tiling is shown in Figure 1.1.1.

If one does not insist that the tiles are polygons, one can turn the inflation rule (1.1.1) into a *stone inflation* [AO1, p. 148]. Parts of the boundary of the prototile will then be turned into fractals. The corresponding stone inflation is given by



and is clearly mutually locally derivable (MLD) with the inflation (1.1.1); see [AO1, Sec. 5.2] for background on MLD as an equivalence relation.

The boundary of the prototile is not a ‘proper’ fractal, in the sense that its Hausdorff dimension is 1. This can be seen by employing the methods described in [46]. Denote the upper part of the boundary of the prototile by

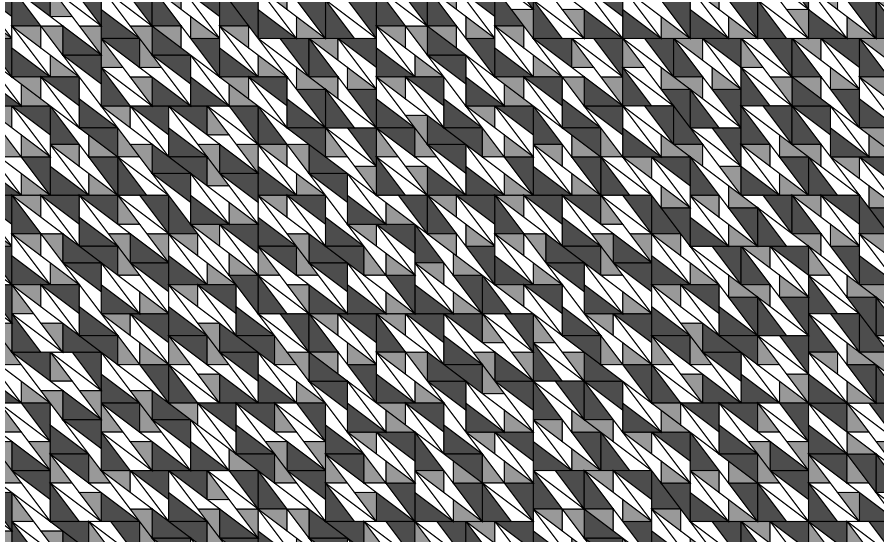


FIGURE 1.2.1. A patch of an inflation tiling generated by the inflation rule (1.2.1). Here, $\mu = \sqrt{\lambda^2 + 1}$, where two of the triangles are right-angled.

Fault lines are a typical phenomenon of non-FLC tilings. In fact, it is shown in [14] (in the proof of Thm. 4.4) that primitive stone inflations either produce FLC tilings or tilings with a fault line. Some non-trivial sufficient conditions for inflation tilings to have FLC are given in [16] and [14].

1.2. One-parameter families of inflation rules

Usually, inflation rules are rigid in the sense that one cannot continuously deform the tiles without destroying the inflation property. Here, we discuss a different example of an inflation rule due to Danzer. It contains one continuous parameter which determines the shapes of the tiles. It can be found in the extended version of a paper by Goodman-Strauss [28], which is available from his website.¹

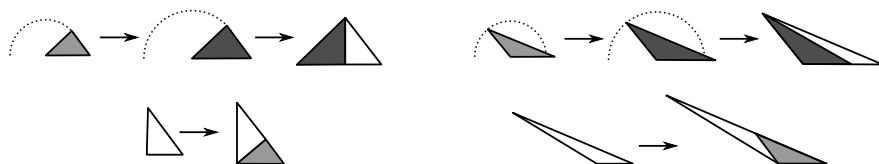
We consider the following inflation rule for three triangular prototiles

$$(1.2.1) \quad \begin{array}{c} \mu \\ \triangle \\ \lambda \end{array} \rightarrow \begin{array}{c} \lambda\mu \\ \triangle \\ \lambda^2 \end{array} \rightarrow \begin{array}{c} \lambda^2\mu \\ \triangle \\ \lambda \quad 1 \end{array} \quad \begin{array}{c} \lambda\mu \\ \triangle \\ 1 \end{array} \rightarrow \begin{array}{c} \triangle \\ \lambda\mu \end{array}$$

where μ is a free parameter. Figure 1.2.1 shows a patch of a tiling arising from this inflation rule. The inflation factor $\lambda \approx 1.3247$ is the largest root of the polynomial $x^3 - x - 1$. It is the smallest Pisot–Vijayaraghavan (PV) number,

¹<http://comp.uark.edu/~strauss/>

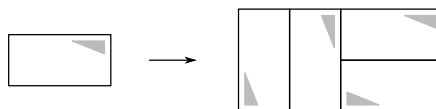
sometimes called the ‘plastic’ number; compare [AO1, Ex. 2.17]. The value of μ can be chosen arbitrarily from the open interval $(\lambda - 1, \lambda + 1)$. Equivalently, the interior angle in the lower left vertex of the small triangle (leftmost in the inflation rule (1.2.1)) can be chosen arbitrarily from the interval $(0, \pi)$. In particular, we can produce tilings with arbitrarily ‘thin’ tiles in this way. The inflation rules for two further choices of μ are shown below. On the left, a realisation with three right-angled triangles is shown, while on the right the inflation uses three obtuse triangles.



Continuously decreasing or increasing the value of μ corresponds to moving the upper vertex of the first two prototiles along the half-circles indicated by dashed arcs. The upper vertex of the third prototile then moves on a different conic section. We leave it to the reader to work out the details of the latter (which is an ellipse).

1.3. A tiling with non-unique decomposition

A close relative of the table tiling (see [42] or [AO1, Ex. 6.2] for the latter) is the tiling defined by the inflation rule



If one ignores the triangular marks in the diagram, the inflated tile has less symmetry than the prototile. Hence, without the triangular marks, the diagram does *not* define an inflation uniquely. As a consequence, the tiling with unmarked tiles violates local recognisability and thus does *not* possess a *local inflation deflation symmetry* (LIDS) in the sense of [AO1, Def. 5.16]. This is indicated in the right-hand part of Figure 1.3.1.

The tiling with triangular marks does have an LIDS, as it ought to have, according to the following result by Solomyak.

Theorem 1.3.1 ([50, Thm. 1.1]). *A self-affine tiling that has FLC with respect to translations has the unique composition property if and only if it is non-periodic.* \square

In our terminology, a self-affine tiling is an FLC tiling originating from a primitive stone inflation, and the unique composition property refers to

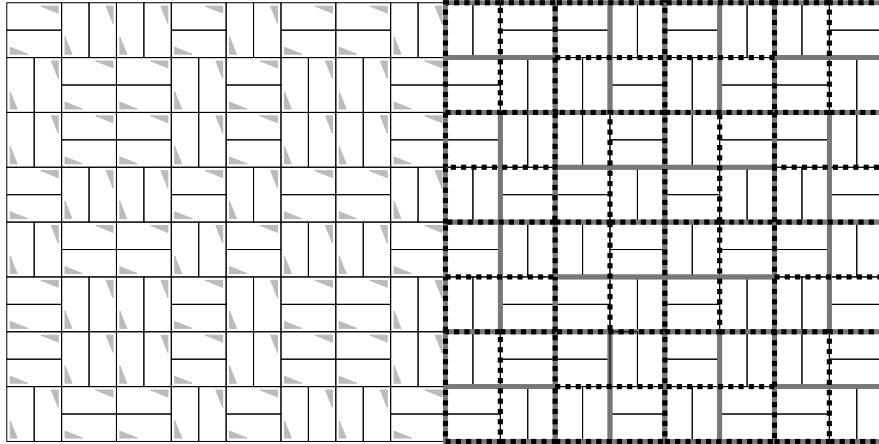


FIGURE 1.3.1. If one ignores the triangular marks in this aperiodic tiling, it has more than one possible preimage under the inflation rule. Two preimages are indicated in the right part of the figure, supertiles of one possibility with grey lines, supertiles of the other with dashed lines.

the LIDS. More precisely, the unique composition property in [50] does not require the supertiles to be determined locally. For the example at hand, this makes no difference. The tilings (marked as well as unmarked) are easily seen to be non-periodic (and hence aperiodic), either by applying Theorem 1.3.1 or by superimposing a hierarchical pattern of squares as in [AO1, Ex. 5.11]; see also [AO1, Fig. 6.50]. This example was discussed by Goodman-Strauss in [27]; see also the extended version of [28] mentioned previously.

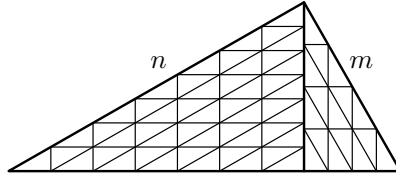
1.4. Überpinwheel

The classical *pinwheel tiling* (see [AO1, Sec. 6.6] and references therein) is an inflation tiling that fails to have FLC with respect to translations, though it has FLC with respect to rigid motions. The tiles in the pinwheel tiling are all congruent (the prototile being a right-angled triangle with edge lengths 1, 2 and $\sqrt{5}$), but they appear in (countably) infinitely many different orientations throughout the tiling. Hence, in order to specify the exact position of some tile in the pinwheel tiling, one needs three parameters with an infinite set of values rather than two; namely, two parameters for the position of its right-angled vertex, say, and one parameter in the circle \mathbb{S}^1 for the orientation of the tile. In the sequel, we will often identify the circle with the half-open interval $[0, 2\pi)$. The latter parameter describes the integer multiples of an irrational rotation angle, so is of the form $n\alpha \bmod 2\pi$, where $\alpha = 2 \arctan(\frac{1}{2})$.

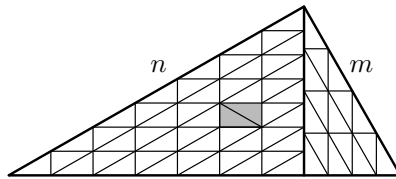
Lorenzo Sadun [44] asked whether there are planar inflation tilings that require two parameters to specify the orientation of the tiles, in the sense that

there are two rationally independent, irrational rotation angles in a tiling. We are now going to discuss an example of such an ‘überpinwheel’ inflation tiling.

The pinwheel inflation rule is generalised as follows. Let T be a right-angled triangle with edge lengths $m, n, \sqrt{m^2 + n^2} =: \lambda$, where $m, n \in \mathbb{N}$ with $m \neq n$. The classical pinwheel tiling corresponds to the case $m = 1$ and $n = 2$ (or $m = 2$ and $n = 1$). There is a canonical partition of λT into congruent copies of T :

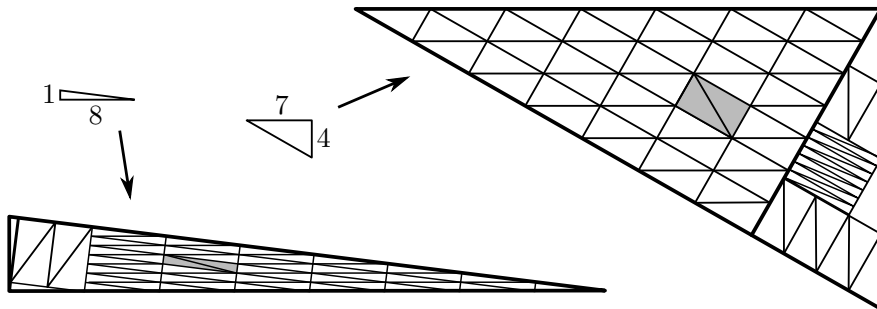


In order to define an inflation rule for an aperiodic tiling with infinitely many orientations, we need to flip at least one (but not all) of the rectangles, for instance as in



Choose an integer N such that $N = \lambda^2 = m^2 + n^2 = k^2 + \ell^2$ for $k, \ell, m, n \in \mathbb{N}$ with $m \neq n, k \neq \ell$ and $\{m, n\} \neq \{k, \ell\}$. Let us take the smallest choice, which is $N = 65 = 1^2 + 8^2 = 4^2 + 7^2$. Let T_1 be a right-angled triangle with edge lengths $1, 8, \sqrt{65}$ and let T_2 be a right-angled triangle with edge lengths $4, 7, \sqrt{65}$.

Consider the pinwheel-like inflation described above, applied to both triangles T_1 and T_2 , but in a ‘coupled’ way. In order to combine these two inflations, replace a rectangular patch of size 7×8 in $\sigma(T_1)$ by a 7×8 rectangular patch of copies of T_2 , and vice versa. One possible way to do so is the following:



The next result shows that each tile in the resulting tilings needs two parameters to specify its orientation.

Theorem 1.4.1. *The angles $\arctan(\frac{1}{8})$ and $\arctan(\frac{4}{7})$ are both irrational, and are independent over \mathbb{Q} .*

PROOF. The irrationality of $\arctan(\frac{1}{8}) = \frac{\pi}{2} - \arccos(\frac{1}{\sqrt{65}})$ follows from the fact that $\arccos(\frac{1}{\sqrt{n}}) \notin \pi\mathbb{Q}$ for $n \geq 3$ odd; see for instance [1, Thm. 3]. This can be proved alternatively using cyclotomic fields. We will illustrate this with $\arctan(\frac{4}{7})$.

If $\arctan(\frac{4}{7}) \in \pi\mathbb{Q}$, then there is an $n \in \mathbb{N}$ such that $(7 + 4i)^n \in \mathbb{R}$, or equivalently there is an $n \in \mathbb{N}$ such that $\frac{7+4i}{|7+4i|}$ is a (complex) n -th root of unity. Then, $\frac{(7+4i)^2}{|7+4i|^2} = \frac{7+4i}{7-4i}$ is also a root of unity. Since $\frac{7+4i}{7-4i} \in \mathbb{Q}(i)$, and the roots of unity in $\mathbb{Q}(i)$ are $\{1, i, -1, -i\}$ [AO1, Sec. 2.5.2], this yields a contradiction. (More generally, all roots of unity in $\mathbb{Q}(e^{2\pi i/n})$ are of the form $\pm e^{2\pi i/n}$; see [54, Exc. 2.3] or [AO1, Sec. 2.5.2].)

The independence of $\arctan(\frac{1}{8})$ and $\arctan(\frac{4}{7})$ can again be shown by interpreting them as complex numbers. If $\arctan(\frac{1}{8})$ and $\arctan(\frac{4}{7})$ were dependent over \mathbb{Q} , then there would exist $k, m \in \mathbb{Z} \setminus \{0\}$ such that $k \arctan(\frac{1}{8}) = m \arctan(\frac{4}{7})$. With $z := \frac{8+i}{|8+i|}$ and $y := \frac{7+4i}{|7+4i|}$, this implies that $z^k = y^m$, hence $z^{2k} = y^{2m}$, which gives

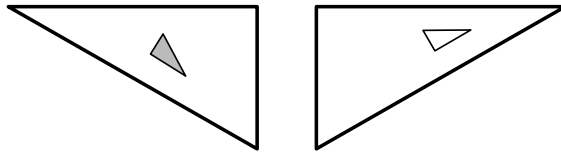
$$\frac{(8+i)^k}{(8-i)^k} = \frac{(7+4i)^m}{(7-4i)^m} \quad \text{and thus} \quad (8+i)^k(7-4i)^m = (8-i)^k(7+4i)^m.$$

Because the ring $\mathbb{Z}[i]$ of Gaussian integers is a unique factorisation domain, the prime factorisation is unique up to units in $\mathbb{Z}[i]$, hence

$$(-i)^k(1+2i)^k(3+2i)^k(1-2i)^m(3+2i)^m = i^k(1-2i)^k(3-2i)^k(1+2i)^m(3-2i)^m$$

and thus $(1+2i)^{k-m}(3+2i)^{k+m} = (1-2i)^{k-m}(3-2i)^{k+m}$. Since $1+2i$, $1-2i$, $3+2i$ and $3-2i$ are pairwise coprime in $\mathbb{Z}[i]$, this yields a contradiction. \square

The fact that copies of both T_1 and T_2 occur in $\sigma(T_1)$ as well as in $\sigma(T_2)$ implies the primitivity of σ . Furthermore, the fact that $\sigma(T_2)$ contains two copies of T_2 that are reflected in their shortest edge ensures that the tiles in the corresponding tilings appear in infinitely many orientations. Indeed, substituting these two tiles yields two copies of T_2 that are rotated against each other by $2 \arctan(\frac{4}{7})$,



Consequently, higher level supertiles contain copies of T_2 that are rotated against each other by an angle of $n \cdot 2 \arctan(\frac{4}{7})$ for all $n \in \mathbb{Z}$. Since we have $\arctan(\frac{4}{7}) \notin \pi\mathbb{Q}$, these angles are distinct. In fact, whenever such a situation occurs, the angles are even uniformly distributed in $[0, 2\pi)$ by [19, Prop. 3.4 and Thm. 6.1]. This result is due to Radin [41] for the pinwheel tiling, while the general case is treated in [19].

Theorem 1.4.2 ([19, Prop. 3.4 and Thm. 6.1]). *Let σ be a primitive inflation rule in \mathbb{R}^2 . Each tiling in the hull of σ has statistical circular symmetry if and only if there is a level- n supertile (for some $n \geq 1$) containing two copies of the same prototile which are rotated against each other by some angle $\alpha \notin \pi\mathbb{Q}$.* \square

Here, statistical circular symmetry means that the orientations of the tiles are not only dense on the circle, but actually uniformly distributed. Since there are countably infinitely many orientations of tiles in the pinwheel tiling, the uniform distribution property refers to frequencies of tiles with an orientation within certain intervals. Uniform distribution then means that, for any two such intervals of the same length, the frequencies of tiles with orientations in these intervals are equal; see [AO1, Sec. 7.1] for a more precise definition.

Via similar constructions, one may obtain examples of tilings in which the orientations of tiles are described by $M > 2$ irrational angles. This can be done by mixing M pinwheel-like inflations with common inflation factor $\lambda = \sqrt{q}$, where q can be expressed as a sum of two distinct squares in M different ways. Nevertheless, illustrating these examples will be inconvenient, due to the inevitably large inflation factors. The next values are given by $325 = 1^2 + 18^2 = 6^2 + 17^2 = 10^2 + 15^2$ for $M = 3$, by $1105 = 24^2 + 23^2 = 31^2 + 12^2 = 32^2 + 9^2 = 33^2 + 4^2$ for $M = 4$, and by $5525 = 55^2 + 50^2 = 62^2 + 41^2 = 70^2 + 25^2 = 71^2 + 22^2 = 73^2 + 14^2 = 74^2 + 7^2$ for $M = 6$; compare entry A052199 in the OEIS [48].

1.5. Tile orientations with distinct frequencies

The classical pinwheel tiling and its relatives discussed above have the slightly surprising property that the tile orientations are uniformly distributed on the circle. A related result holds for tilings that have FLC with respect to translations.

Theorem 1.5.1 ([20, Thm. 2.3]). *Let σ be a primitive inflation rule such that the tilings in the hull of σ have FLC. If, for any two congruent tiles S and T , the patch $\sigma(S)$ is congruent to the patch $\sigma(T)$, the frequencies of congruent tiles with different orientations are equal.* \square

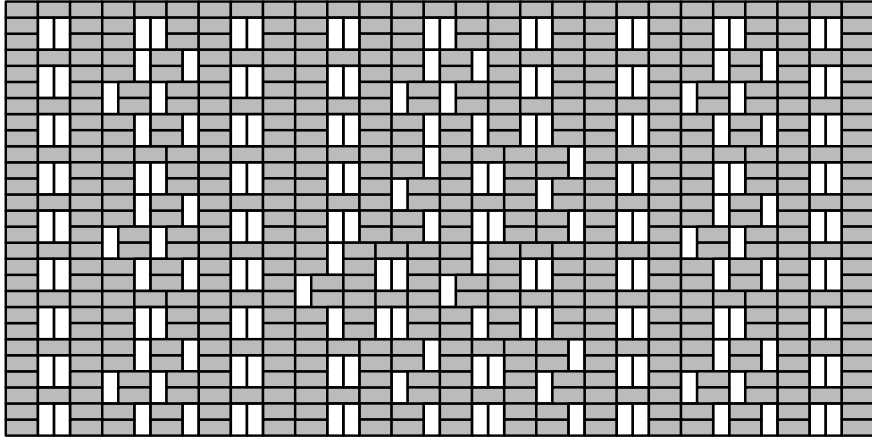


FIGURE 1.5.1. A level-3 inflation patch of the aperiodic ‘punch card’ tiling (without markers), in which horizontal tiles are more frequent than vertical ones. This requires different inflation rules for horizontal and vertical rectangles, as specified in Eq. (1.5.1).

Note that, throughout [AO1] and thus far in this chapter, we have tacitly taken the compatibility of inflation and rotation for granted. That is, we have implicitly assumed the condition of Theorem 1.5.1 to be satisfied. For instance, if the inflation rule of the Ammann–Beenker tiling is specified by showing the inflation of a square T as $\sigma(T)$, then we implicitly assumed that T rotated by $\pi/2$ is substituted by the patch $\sigma(T)$ rotated by $\pi/2$. However, this need not be the case in general. In order to construct a tiling where, say, horizontal rectangles are more frequent than vertical ones, one needs to specify two different inflation rules for vertical and horizontal rectangles. The following example defines such a rule,

$$(1.5.1) \quad \begin{array}{c} \text{Horizontal rectangle} \\ \rightarrow \\ \begin{array}{|c|c|c|} \hline \text{Grey} & \text{White} & \text{Grey} \\ \hline \text{Grey} & \text{White} & \text{Grey} \\ \hline \text{Grey} & \text{White} & \text{Grey} \\ \hline \end{array} \end{array} \quad \begin{array}{c} \text{Vertical rectangle} \\ \rightarrow \\ \begin{array}{|c|} \hline \text{Grey} \\ \hline \text{White} \\ \hline \text{Grey} \\ \hline \end{array} \end{array}$$

We refer to the corresponding tilings as ‘punch card’ tilings. A patch is shown in Figure 1.5.1. It obviously contains more horizontal rectangles than vertical ones. More precisely, since the inflation matrix is $M_\sigma = \begin{pmatrix} 7 & 6 \\ 2 & 3 \end{pmatrix}$ with PF eigenvalue 9 and corresponding right eigenvector $(\frac{3}{4}, \frac{1}{4})^T$, there are three times as many horizontal as vertical rectangles in any tiling of the hull.

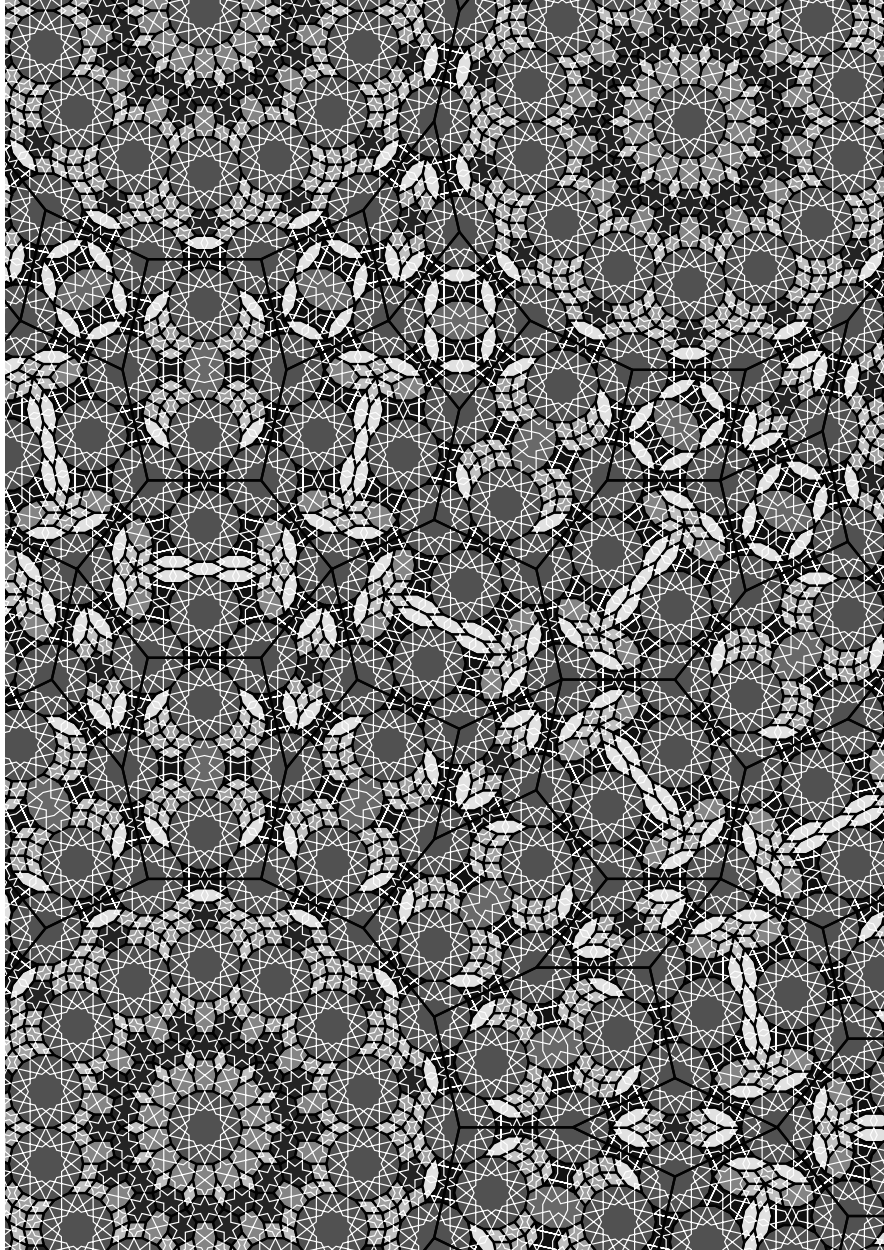


FIGURE 1.6.1. An inflation tiling due to Pautze [40] with 14-fold dihedral symmetry using prototiles inspired by Islamic girih tiles. Level-1 supertiles are indicated by thicker black lines. White lines serve as decoration only.

1.6. Tilings inspired by girih tiles

Many amateur mathematicians have been attracted to inflation tilings, and have devised many new constructions. Some have even substantially influenced the development of the subject, such as, for instance, Robert Ammann [45] and Joan Taylor [49]. The Tilings Encyclopedia [21] further contains examples by Ernesto Amezcua, Laurenz Andritz, Tjipke Hibma, Dale Walton and others; see also the work of Markus Rissanen and Jarkko Kari [32] as well as that of Kurt Hofstetter and the author of this chapter [22].

Several of the constructions are relatively easy to devise, via polyominoes, tangram pieces, or other simple shapes as prototiles. Some of the constructions are considerably more sophisticated. These include inflation tilings inspired by *girih patterns*,² which are sophisticated designs in Islamic architecture; see for instance [5] and references therein. While girih patterns usually are not true inflation tilings, the Tilings Encyclopedia [21] contains examples of proper inflation tilings that are based on similar building blocks.

In Figure 1.6.1, we show an example based on 7-fold variants of girih tiles. This inflation tiling is due to Stefan Pautze [40]. Its inflation rule requires the rather large inflation factor $2 + 4 \cos(\frac{\pi}{7}) + 2 \cos(\frac{2\pi}{7}) \approx 6.851$. For this reason, the image only shows a patch of the tiling where some supertiles (and hence the inflation rule) are indicated by bold lines. In particular, there are eleven prototiles altogether, namely two rhombuses, three convex hexagons, two octagons (one convex and one non-convex), three decagons (two convex and one non-convex) and one regular 14-gon. All but the convex octagon occur in Figure 1.6.1. The level-1 supertiles in the figure are indicated by bold black lines. Only supertiles of the two rhombuses, of two of the hexagons, and of the 14-gon are shown. However, it is not too hard to reconstruct the other supertiles, by taking into account that all supertile edges look the same — they are all bisecting a patch consisting of the sequence (14-gon, non-convex decagon, 14-gon) — and that all supertiles have the same symmetries as the prototiles (in most cases, two orthogonal axes of mirror symmetry).

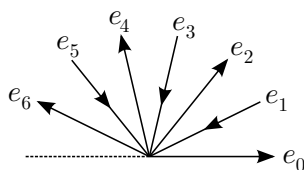
1.7. Cyclotomic rhombus tilings

Below, we shall refer to planar aperiodic tilings where all prototiles are rhombuses with interior angles of the form $\frac{k\pi}{n}$ ($n \in \mathbb{N}, 1 \leq k \leq n-1$) as *cyclotomic rhombus tilings*. These seem to arise naturally in various contexts, for instance from cyclotomic cut and project schemes; see [AO1, Sec. 7.3]. However, finding simple inflation rules for cyclotomic rhombus tilings can be

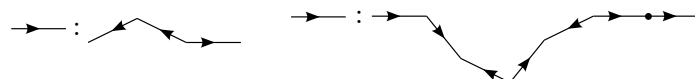
²Girih is Persian for ‘knot’. It refers to decorations in Islamic architecture that are built from interlaced strips, often forming patterns with 6-, 8-, 10- or 12-fold dihedral symmetry.

difficult for larger values of n , such as for $n > 10$, say. In [15], a family of cyclotomic rhombus tilings is obtained by a local derivation from inflation tilings with trapezoids as prototiles. The construction yields cyclotomic rhombus tilings for odd values of $n \geq 5$. In [30], Harriss gives inflation rules for cyclotomic rhombus tilings, again for odd $n \geq 5$. Recently, Pautze found several constructions that result in cyclotomic rhombus tilings for all $n \geq 5$ [40]. It turns out that it is particularly difficult to find consistent inflation rules for the thinnest prototiles (with interior angles $\frac{\pi}{n}$ or $\frac{2\pi}{n}$), where consistency means that no gaps and no overlaps occur when the inflation rule is iterated.

One reason for this difficulty is that there are no interesting stone inflations for rhombuses — dissecting rhombuses into smaller rhombuses only yields trivial dissections, and if all edges have unit length, the inflation factor is always an integer. Hence, one needs inflation rules in which supertiles have protrusions (or bumps) and indentations (or dents); compare the familiar inflation rule for Penrose rhombus tilings; see [11, Fig. 11] or [21]. In a recent paper, Maloney [36] presents a remarkably simple idea which solves this problem for odd values of n . The prototiles are equipped with orientations (indicated by arrows in the figures below). If an edge is parallel to one of the vectors $e_k = (\cos(\frac{k\pi}{n}), \sin(\frac{k\pi}{n}))^T$ for even k , then it is given the same orientation as e_k , otherwise (for odd k) the opposite orientation. Eq. (1.7.1) shows the situation for $n = 7$,

(1.7.1) 

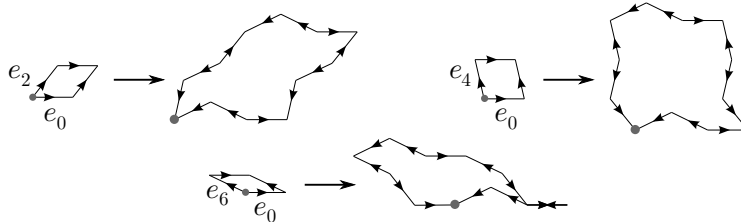
One can then define an edge substitution as follows. An edge in direction e_0 is substituted by a zigzag path of edges in the directions of the e_k . For instance, an edge in direction e_0 can be substituted by an edge sequence $(e_1, -e_6, e_0)$ (left part of Eq. (1.7.2) below), or by $(e_0, -e_5, -e_6, e_2, e_1, e_0, e_0)$ (right part),

(1.7.2) 

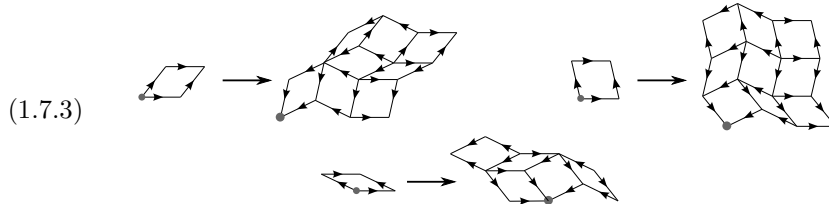
Note that, as shown in this example, an edge $-e_k$ points in the opposite direction as e_k , but the direction of the arrow is *not* reversed. For simplicity, one requires that the sequence can be partitioned into pairs $\{-e_k, e_{n-k}\}$ (with $1 \leq k \leq n - 1$), plus an arbitrary number of e_0 directions. This condition implies that the starting point and the endpoint of the sequence lie on the same horizontal line. Rotated edges e_k are substituted by the corresponding

rotated edge sequences. For odd values of k , the orientations of all the arrows are reversed.

This edge rule translates into a skeleton for the inflation of the rhombuses. The four edges of a rhombus with edges in direction e_0 and e_k (with k even) are substituted by the corresponding four edge paths. For instance, for $n = 7$, there are three such rhombuses. Choosing the left edge sequence in Eq. (1.7.2) produces the following partial inflation,



Any edge sequence that yields non-crossing closed edge paths in this manner may be used to define an inflation rule for cyclotomic rhombus tilings. Note that, in the example above, there is one pair of edges that coincide, in the right part of the partial inflation of the bottom tile. In this case, the two edges cancel each other, and will be omitted. By a theorem of Kannan–Soroker [31] and Kenyon [34], the area enclosed by the edge path can be tiled by rhombuses. In general, there are several possibilities to do so. Here, we show one possible way of extending the partial inflation above to an inflation rule:



In each step of the construction, one requires that the orientations of edges follow the rule of (1.7.1). Note that the inflation rule diagram above seems to be ambiguous: The prototiles are mirror symmetric, whereas the level-1 supertiles are not. Usually, one breaks the mirror symmetry in the diagram by some markings, as in the example of Section 1.3. This way, the prototiles are given a *chirality*; compare the similar situation for the Lançon–Billard tiling [AO1, Sec. 6.5.1]. Here, the rule is made consistent by the implicit convention that all chiralities in the diagram are the same (that means, reversing the orientation of the arrows corresponds to a rotation of the tile, not to a reflection). As one can check, this implies that tiles of *one* chirality suffice to construct a tiling of the plane, so there is no need to actually draw these additional markings. This chiral inflation rule thus produces a consistent

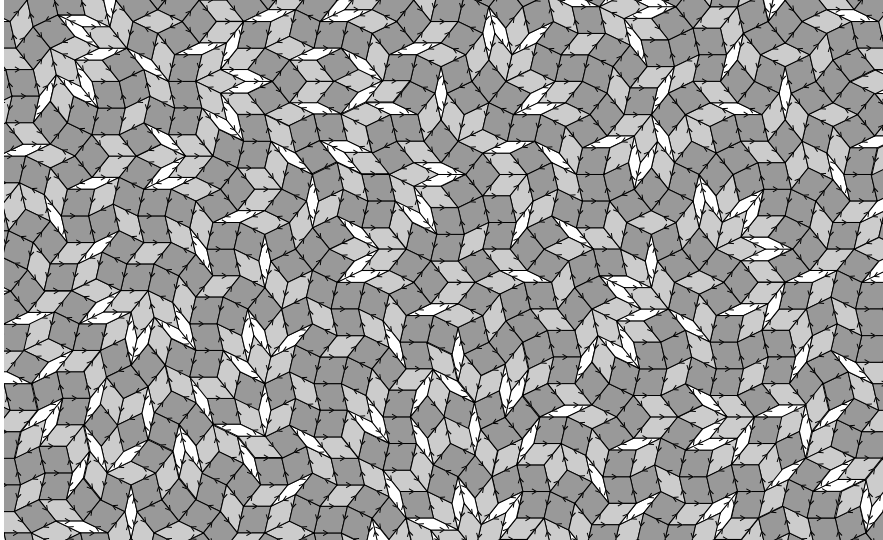


FIGURE 1.7.1. A patch of the cyclotomic rhombus tiling for the inflation rule specified in Eq. (1.7.3).

orientation of the edges in the tilings. Hence, neither gaps nor overlaps will occur for this inflation rule. Figure 1.7.1 shows a patch for this example.

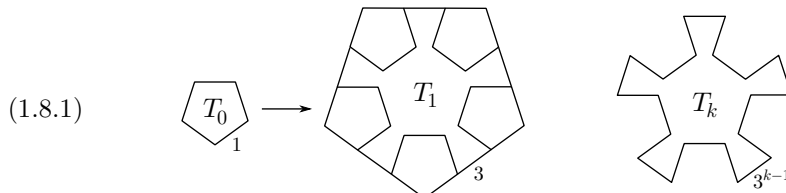
Along similar lines, one aim of [36] was to find inflation rules for cyclotomic rhombus tilings such that not only the hull is invariant under rotation by $\frac{2\pi}{n}$, but that also an individual fixed point tiling is itself invariant. A computer-aided search found an inflation rule of the kind described above for a tiling with 11-fold rotational symmetry. The corresponding edge sequence has length 35, and the inflation factor is approximately 27.2004; see [36] for further details.

Recently, Kari and Rissanen [32] found inflation rules for cyclotomic rhombus tilings with $2n$ -fold rotational symmetry, for arbitrary values of n . Their construction is also based on appropriate edge substitution rules. Here, the edge substitution is made consistent by letting the edges of the supertiles bisect identical sequences of rhombuses which are invariant under rotation by π . In this way, the orientation of edges no longer plays a role. All edge pairs are consistent in the sense that neither gaps nor non-coinciding overlaps occur. The inflation rules are then chosen such that, at the vertices of the supertiles, only tiles with the smallest interior angle $\frac{\pi}{n}$ meet. In the resulting tilings, each supertile vertex is then surrounded by a star that comprises $2n$ rhombuses. This construction yields a fixed point of the inflation with individual $2n$ -fold rotational symmetry. For $n = 11$, the inflation factor of this construction is approximately 48.871.

Independently, Pautze described a plethora of inflation rules for cyclotomic triangle tilings and rhombus tilings with n -fold symmetry [40], using smaller (but still generally large) inflation factors.

1.8. Infinitely many prototiles

There are examples of inflation tilings that use finitely many tile shapes up to similarity, but infinitely many prototiles up to congruence. One example emerged in answer to the question of whether there is a tiling of the plane in which all tiles are fivefold symmetric [8]. These tilings are required to be locally finite [AO1, Def. 5.3], and the tiles to be topological disks. It turns out that the answer is affirmative if the tiles are allowed to be arbitrarily large. The following inflation rule provides an example,



Here, the prototiles have two distinct shapes. The prototile T_0 is a regular pentagon of unit edge length. The tiles T_k ($k \in \mathbb{N}$) are non-convex, fivefold symmetric 20-gons where all edges have length 3^{k-1} . The inflation $\sigma(T_0)$ is indicated in the figure above, it consists of T_1 and five copies of T_0 . For $k \geq 1$, let $\sigma(T_k) = T_{k+1} = 3T_k$. This inflation is clearly not primitive: Firstly, no $\sigma^n(T_1)$ contains a copy of T_0 , and secondly, there are infinitely many prototiles. Due to the non-primitivity, pathological behaviour may occur. For instance, if we attempt to construct a fixed point tiling by starting from T_1 centred at the origin and applying the inflation, the resulting sequence $T_1, \sigma(T_1), \sigma^2(T_1), \dots$ converges to ‘a single infinite tile’. Nevertheless, the supertiles $\sigma^n(T_0)$ can provide a non-trivial fixed point of σ as follows.

The idea is to find a copy of T_0 in the relative interior of $\sigma^2(T_0)$, hence T_0 can serve as a seed for a fixed point. Consider T_0 to be centred at the origin. Choose a pentagon P (a specific copy of T_0) inside $\frac{1}{9}\sigma^2(T_0)$. Banach’s contraction principle applied to this contraction on T_0 yields a fixed point x in the interior of T_0 . Now, consider the translate $T_0 - x$. Then,

$$T_0 - x \subset \sigma^2(T_0 - x) \subset \sigma^4(T_0 - x) \subset \sigma^6(T_0 - x) \subset \dots$$

is a nested sequence that converges in the local topology to a fixed point of the inflation σ . Figure 1.8.1 shows the point x and part of the tiling fixed under the inflation.

Another interesting family of examples with infinitely many prototiles (up to congruence) but finitely many prototiles (up to similarity) is described

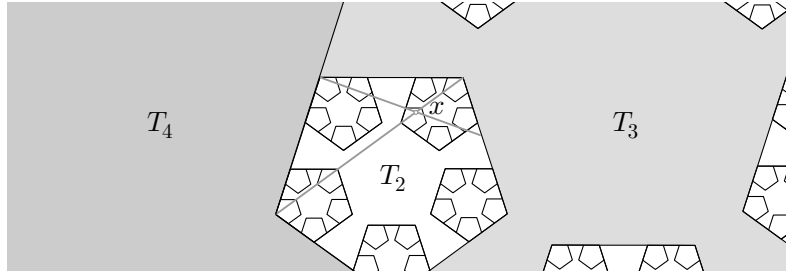
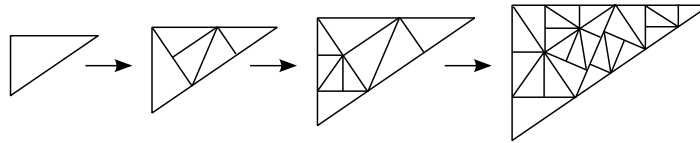


FIGURE 1.8.1. The central patch of a fixed point of the inflation rule (1.8.1) with fivefold tiles. The grey lines indicate how to construct the fixed point x geometrically.

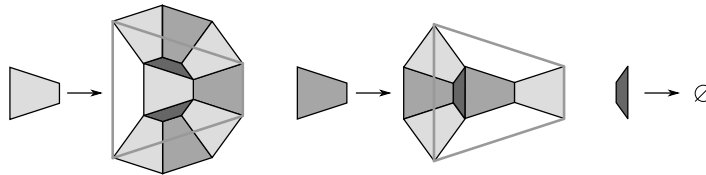
in [43], where Sadun generalises the pinwheel inflation rule to arbitrary right-angled triangles. The rule is that, in each step, the biggest triangles are subdivided topologically according to the pinwheel inflation rule (for the latter, see [AO1, Sec. 6.6]). In the generic case, this construction produces tilings with triangles of infinitely many distinct sizes, which all are similar to each other. The general idea is indicated in the following sketch,



In countably many cases, this construction gives rise to an inflation with finitely many prototiles. In particular, let θ denote the smallest interior angle of the triangle. Then, the inflation rule uses finitely many prototiles if and only if $\frac{\log(\sin(\theta))}{\log(\cos(\theta))} = \frac{p}{q} \in \mathbb{Q}$, with p and q coprime. The number of tile sizes in the tiling is then given by $\max(p, q)$. In the remaining (uncountably many) cases, there are infinitely many prototiles. Even then, the sizes of all prototiles still lie within a certain range [43, Lemma 1], unlike in the fivefold example above, where tiles become arbitrarily large.

1.9. Inflations with an empty supertile

The following inflation rule σ was found by Socolar; see the ‘Birds and Bees’ entry in the Tilings Encyclopedia [21].

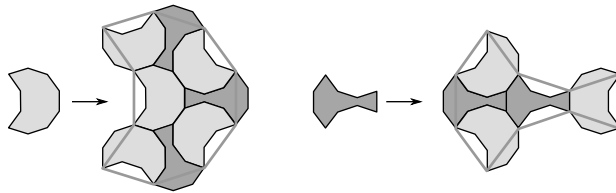


Note that this is not a stone inflation, but still a consistent inflation rule; compare [AO1, Sec. 5.6]. The inflated prototile shape is indicated by the grey lines. This inflation is neither primitive nor even irreducible, because the smallest tile is mapped to the empty set.³ Thus, the corresponding column of the substitution matrix

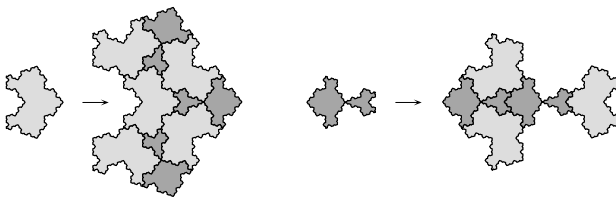
$$M_\sigma = \begin{pmatrix} 5 & 3 & 0 \\ 3 & 2 & 0 \\ 2 & 1 & 0 \end{pmatrix}$$

contains only zeros. Nevertheless, the inflation rule defines a hull which is repetitive and minimal. Since this example is neither primitive nor a stone inflation, the PF eigenvalue of M_σ need not agree with the squared inflation factor. However, here it actually does. The eigenvalues of M_σ are τ^4 , τ^{-4} and 0, where $\tau = \frac{1}{2}(1 + \sqrt{5})$ is the golden ratio. The prototiles have edge lengths 1 and $\tau^2 = \tau + 1$; the inflation factor is τ^2 . So indeed, the PF eigenvalue of the substitution matrix is the squared inflation factor. The right and left PF eigenvectors (up to normalisation) are given by $(\tau^2, \tau, 1)^T$ and $(\tau, 1, 0)$.

In general, although the tile that is replaced by an empty tile may appear superfluous, it may be difficult to find an equivalent inflation (in the sense that it defines a tiling in the same MLD class) for polygonal tiles without including it. In this case, it is easy to see that one can work with the following inflation rule,



Using two prototiles with fractal boundaries, this can be turned into a stone inflation, in the spirit of [AO1, Rem. 6.9]. The resulting inflation rule is



³It is instructive to compare this rule with that for Penrose's $(1 + \varepsilon + \varepsilon^2)$ -tiling, see [AO1, Ex. 5.13], where one tile is mapped to itself, hence primitivity is also violated. The present example pushes this behaviour even further.

This stone inflation has the symmetric inflation matrix $\begin{pmatrix} 5 & 3 \\ 3 & 2 \end{pmatrix}$, with largest eigenvalue τ^4 and corresponding PF eigenvector $(\tau, 1)^T$. This shows that the seemingly meaningless PF eigenvector of the non-primitive matrix above in fact yields the correct inflation factor and correct relative frequencies of the two large prototiles (as well as determining the correct areas of the fractal tiles). Even the vanishing prototile area can be interpreted consistently.

Remark 1.9.1. A close inspection of the ‘fractalised’ inflation rule reveals that the smaller prototile can consistently be split into two prototiles. This would result in an alternative inflation rule σ' with three prototiles, which produces a tiling in the same MLD class. The corresponding inflation matrix reads

$$M_{\sigma'} = \begin{pmatrix} 5 & 2 & 1 \\ 3 & 2 & 0 \\ 3 & 1 & 1 \end{pmatrix}$$

with PF eigenvalue τ^4 as before, and PF eigenvectors proportional to $(\tau, 1, 1)^T$ (for the frequencies, up to normalisation) and $(3\tau + 1, \tau + 1, 1)$ (for the prototile areas). We leave it to the reader to explore the various connections between these inflations, and to determine the Hausdorff dimension of the prototile boundaries (which follows from their structure as Koch-type curves and is given by $\frac{\log(3)}{2 \log(\tau)} \approx 1.1415$). \diamond

Together with the examples of [AO1, Rems. 6.9 and 6.11], this generalised inflation raises two questions. Firstly, it would be interesting to know which proper inflation rules (but possibly with bumps and dents) can be turned, within the same MLD class, into a stone inflation by a change of prototiles, possibly with fractal boundaries. Secondly, one would like to have at least sufficient criteria for when it is possible to replace a generalised inflation rule by a proper one, again under preservation of the MLD class.

1.10. Overlapping tiles

Even though many examples of inflations in [AO1] and in this chapter are actually stone inflations, there are several exceptions, such as the Penrose rhombus tilings [AO1, Sec. 6.2] and the inflation rules for cyclotomic rhombus tilings in Section 1.7. Usually, the non-stone inflations are chosen carefully in such a way that either no overlaps occur at all (bumps of one supertile fill exactly the dents in adjacent supertiles; see for instance the examples in Sections 1.7 and 1.9), or overlapping tiles coincide exactly (such as the Penrose rhombus inflation or Schlottmann’s square triangle inflation described in [AO1, Sec. 6.3.1]). In contrast to this, there are rules where the overlaps do not coincide. For instance, the rule in Eq. (1.10.1), which was found by Petra Gummelt [29], allows non-coincident tile overlaps in order to produce tilings

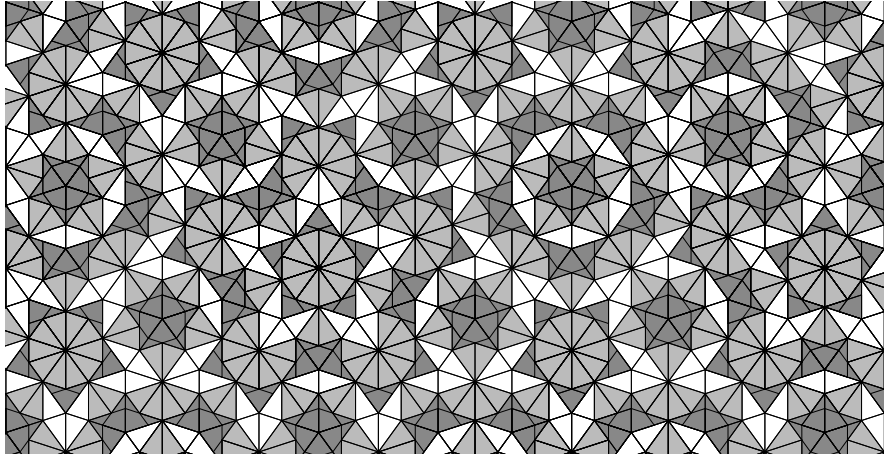
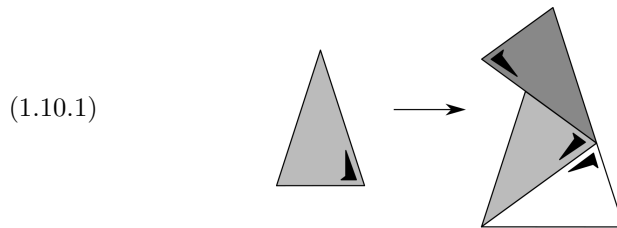


FIGURE 1.10.1. A patch obtained by the overlapping inflation (1.10.1). Note that there is only one kind of overlap, which consists of two dark grey tiles that form a Penrose kite.

with inflation factor $\tau = \frac{1}{2}(1 + \sqrt{5})$ with only one prototile (a stone inflation requires at least two prototiles, since the algebraic degree of τ is two).



The single prototile T is an isosceles triangle with edge lengths 1, τ and τ . The inflation factor is τ , and $\sigma(T)$ consists of three copies of the prototile, with one of them sticking out. This rule is reminiscent of the Penrose triangle inflation; compare [AO1, Fig. 6.2]. For visual reasons, the three tiles in the image above are distinguished by different shades of grey, but all three are of the same type. Iterating the inflation σ yields several overlaps, where the overlapping tiles do not coincide exactly. Keeping track of all edges, respectively of all partial overlaps of tiles, yields the covering illustrated in Figure 1.10.1. It is straightforward to translate this covering into a tiling, by considering the set of all edges and the partition of the plane they define.

The image is to be understood as showing transparent tiles, so no (parts of) tiles are hidden by other tiles. Obviously, there is only one kind of overlap: Two overlapping dark grey tiles form a ‘dart’. This explains the apparent similarity to the Penrose tiling in its kites and darts version. In fact, it is

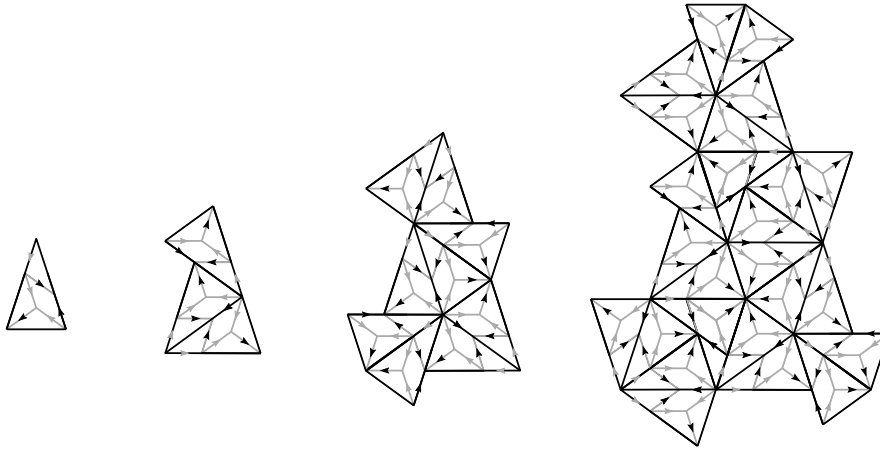
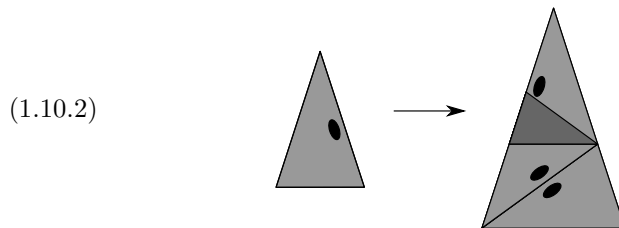


FIGURE 1.10.2. A decoration showing that the overlapping inflation from Eq. (1.10.1) produces tilings that are MLD with Penrose tilings.

not difficult to show that the two versions are MLD, employing the methods described in [AO1, Sec. 6.2]. For instance, via the decoration indicated in Figure 1.10.2, one can establish equivalence with the Penrose rhombus tiling.

Gummelt suggested a similar inflation rule [29] for the golden triangle from above with inflation factor τ , which generates tilings with several different patterns of overlapping tiles,



The inflation again uses three copies of a single prototile, but now two tiles overlap in the interior of the level-one supertile. The overlap is indicated by a darker shading in the rule of (1.10.2). It is less clear whether the tilings generated by this rule are MLD to Penrose tilings. A patch of such a tiling is shown in Figure 1.10.3. Similar constructions using overlaps in non-FLC tilings can produce tilings with infinitely many prototiles.

In the examples above, tiles are considered to be *transparent*, hence all edges of overlapping tiles are visible. In contrast to this, there are also tilings with overlaps where some tiles really hide other tiles, or parts of other tiles; and only this overlay structure leads to an aperiodic pattern. The following example illustrates this idea. It is described in [22], where a similar example

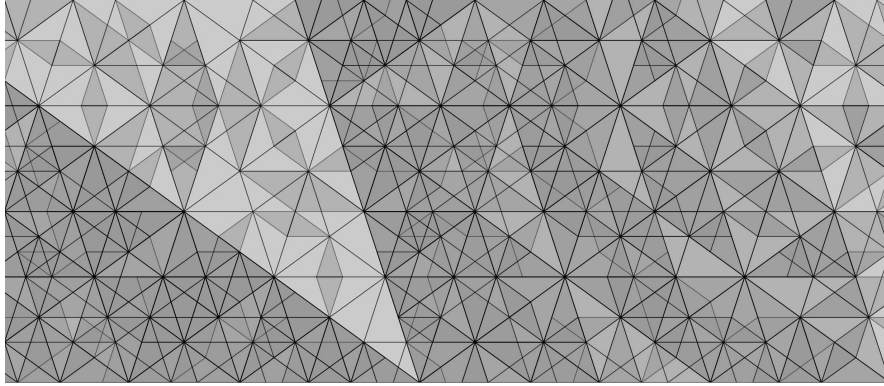


FIGURE 1.10.3. A patch of a tiling generated by the overlapping inflation (1.10.2), with transparent tiles. Darker regions in the tiling correspond to multiple covers in the corresponding covering.

is studied in detail. The construction was found by the artist Kurt Hofstetter, so we refer to such tilings as *Hofstetter tilings*.

The construction proceeds as follows. All tiles are (2×2) -squares. In the first iteration, start from a single square (top of left column in Figure 1.10.4), then place a second square, rotated counterclockwise by $\frac{\pi}{2}$ with respect to the first one, translated by $(1, 1)^T$, such that it lies below the first square (second entry in left column). Place a third square, rotated by $\frac{\pi}{2}$ and translated by $(1, -1)^T$ with respect to the second one, below the second square (third entry in left column). A fourth square, rotated by $\frac{\pi}{2}$ and translated by $(-1, -1)^T$

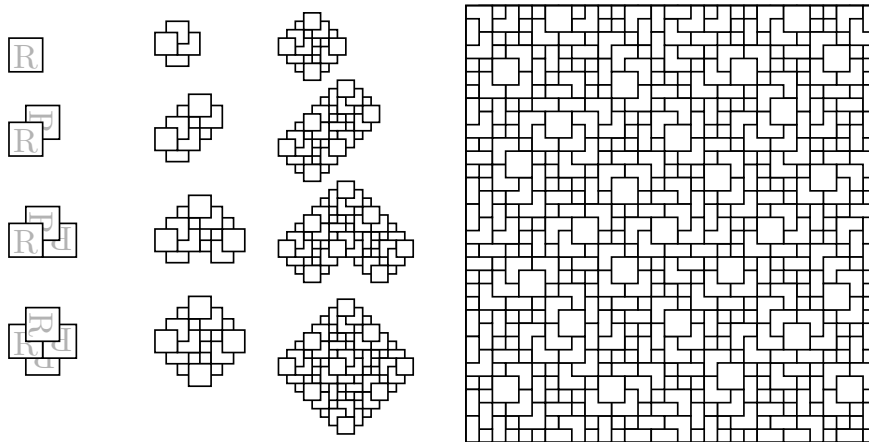


FIGURE 1.10.4. First iterations (four steps each) for generating a Hofstetter tiling (left columns) and a patch of a resulting tiling (right).

with respect to the third square, is placed below the third (and first) square (bottom entry). This constellation of four squares is the building block B_1 for the next generation (second column in Figure 1.10.4). Now repeat the above steps where ‘square’ is replaced by ‘copy of B_1 ’ and the translation vectors $(\pm 1, \pm 1)^T$ by $(\pm 2, \pm 2)^T$ (as shown in the second column). The resulting constellation is denoted B_2 . More generally, repeat the same steps for B_i and translation vectors $(\pm 2^i, \pm 2^i)^T$.

The resulting constellations B_n are not patches, but coverings of (part of) the plane. Some of the squares in this covering are covered partially by other squares, a few squares are covered completely. In fact, the covering degree of the resulting coverings is 2 almost everywhere, except close to the boundary of the B_n . In order to translate this into a tiling, we simply omit the covered parts. Since the central part of B_i occurs in the centre of B_{i+1} (for $i \geq 3$) the sequence of the B_i converges to a fixed point of the iteration, in the standard local topology.

The examples studied so far [22] are MLD to certain inflation tilings. Nevertheless, similar approaches might yield tilings that are not easily generated by inflations.

1.11. Tiles from automorphisms of the free group

One particular construction of inflation tilings employs automorphisms of the free group F_n with n generators (represented by letters) [53]. Several particular examples have been studied; see for instance [4, 2]. Nevertheless, this method seems less flexible than the inflation method, as most of the inflation tilings described here and in [AO1] cannot be obtained in this way. We describe the general method by using a particular example of Kenyon [35]. This is probably one of the earliest examples of this kind to be found in the literature (but compare the lecture notes [53] for more).

Consider the free group F_3 over 3 letters $\{a, b, c\}$. Let $\Phi \in \text{Aut}(F_3)$ be defined by

$$(1.11.1) \quad \Phi(a) = b, \quad \Phi(b) = c, \quad \Phi(c) = ca^{-1}b^{-2}.$$

Its image under Abelianisation is the matrix $M_\Phi \in \text{GL}(3, \mathbb{Z})$ given by

$$M_\Phi = \begin{pmatrix} 0 & 0 & -1 \\ 1 & 0 & -2 \\ 0 & 1 & 1 \end{pmatrix};$$

see [AO1, Sec. 4.1] for some background. The characteristic polynomial is $p(x) = \det(x\mathbb{1} - M_\Phi) = x^3 - x^2 + 2x + 1$, which is irreducible over \mathbb{Q} . Let λ be the (unique) non-real root of p with positive imaginary part. Hence, λ is approximately $0.696 + 1.435i$. This λ acts as our inflation factor. More

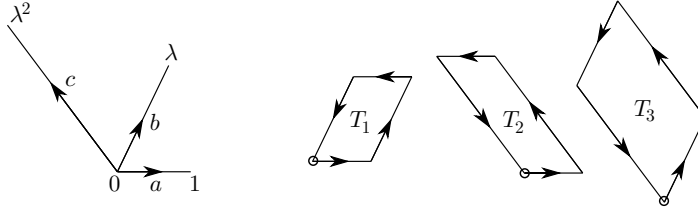
precisely, since it is a (non-real) complex number, it is considered to act in the complex plane, hence it acts as a scaling followed by a rotation. Since $\lambda \cdot 1 = \lambda$, $\lambda \cdot \lambda = \lambda^2$ and $\lambda \cdot \lambda^2 = \lambda^2 - 2\lambda - 1$, which matches the left eigenvector relation

$$(1, \lambda, \lambda^2)M_\Phi = \lambda(1, \lambda, \lambda^2),$$

we may identify a with 1, b with λ , and c with λ^2 . More precisely, we consider a , b and c as the *oriented* line segments from 0 to 1, from 0 to λ , and from 0 to λ^2 , respectively. Then, the free group commutators

$$aba^{-1}b^{-1}, \quad aca^{-1}c^{-1} \quad \text{and} \quad bcb^{-1}c^{-1}$$

correspond to closed paths. These paths (more precisely, the parallelograms T_1 , T_2 and T_3 bounded by them) become our prototiles, where the reference position of each parallelogram is its lower left resp. its lowest vertex point,



The action of Φ on the edges now defines the inflation rule as follows. Since T_1 corresponds to $aba^{-1}b^{-1}$, the relation $\Phi(aba^{-1}b^{-1}) = bcb^{-1}c^{-1}$ means that T_1 is directly mapped to T_3 under the inflation, with preservation of the reference point. For T_2 , we get

$$\Phi(aca^{-1}c^{-1}) = bca^{-1}b^{-1}ac^{-1} = (bcb^{-1}c^{-1})ca^{-1}(aba^{-1}b^{-1})ac^{-1},$$

which means that T_2 turns into a patch built from one copy each of T_1 and T_3 (the terms in brackets), with specific relative position as given by the term between the brackets. The last factor corresponds to the return to the initial reference point. Likewise, the inflation of T_3 comes from

$$\begin{aligned} \Phi(bcb^{-1}c^{-1}) &= c^2a^{-1}b^{-2}c^{-1}b^2ac^{-1} \\ &= ca^{-1}(aca^{-1}c^{-1})b^{-1}(bcb^{-1}c^{-1})b^{-1}(bcb^{-1}c^{-1})b^2ac^{-1}, \end{aligned}$$

with interpretation analogous to the above. In general, translates of a prototile correspond to conjugates of the word that represents the prototile. This way, the reference point is always reset to its original position. The inflation

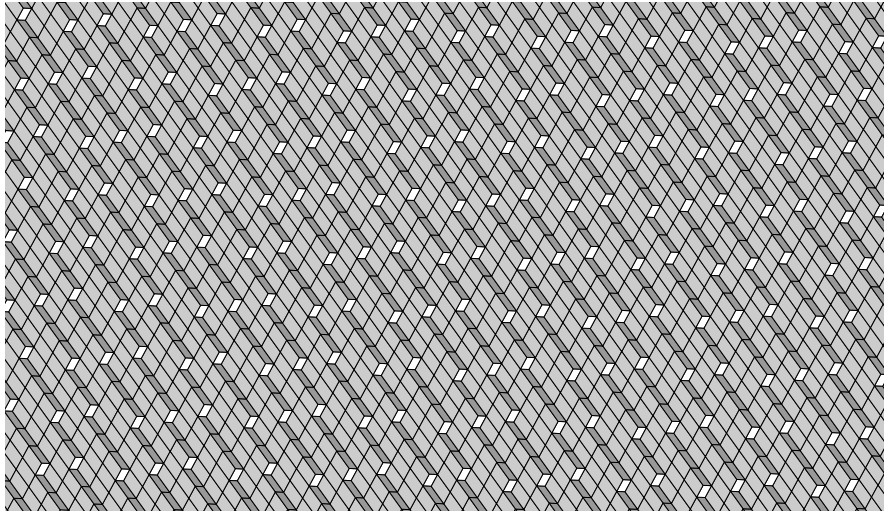
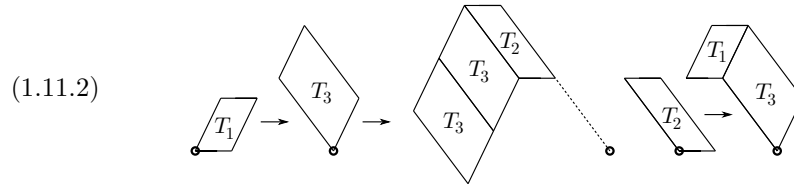


FIGURE 1.11.1. A patch of the inflation tiling with three parallelogram-shaped prototiles, obtained by the rule (1.11.2). The tiling is aperiodic.

for the three prototiles looks as follows,



By construction, each tile type appears in only one orientation in the tiling; compare Figure 1.11.1 for an illustration.

Clearly, this inflation is not a stone inflation. By a standard construction, which is based on the original edge inflation (and is similar to the one used in [AO1, Rem. 6.11]), the inflation (1.11.2) can be turned into a stone inflation with fractally shaped (or bounded) prototiles. The shape of the new tiles is illustrated in Figure 1.11.2. The original parallelograms, in the correct relative positions, are indicated for comparison. Note that the new prototiles have ‘fractal antennas’, which originate from the edge inflation induced by Φ from Eq. (1.11.1). They are the limits of paths that are effectively traversed in both directions. In analogy to the situation of Section 1.7, these antennas can consistently be removed. This corresponds to reducing the edge words as elements within the free group.

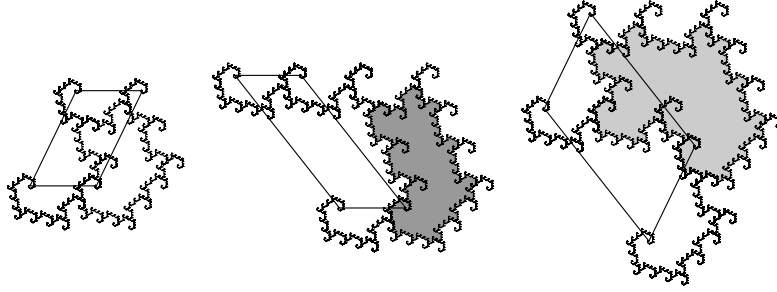
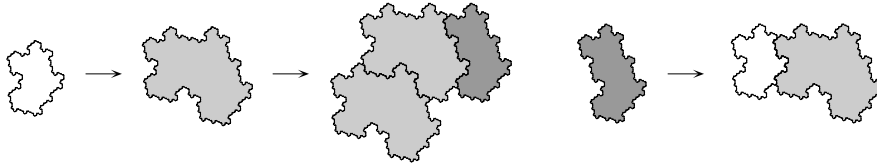


FIGURE 1.11.2. Fractalised versions of the tiles of Eq. (1.11.2).

The induced inflation rule now looks as follows,



where one has to observe that the relative shifts of the fractal tiles with respect to the parallelograms arise as a consequence of the removal of the antennas. This results in a horizontal shift along an edge of type a for T_1 and T_2 , while it means a shift along an edge of type b for T_3 . The inflation matrix is

$$M = \begin{pmatrix} 0 & 1 & 0 \\ 0 & 0 & 1 \\ 1 & 1 & 2 \end{pmatrix},$$

which also applies to the original inflation rule (1.11.2). The PF eigenvalue is the dominant root of $x^3 - 2x^2 - x - 1$, which is approximately 2.5468. Since it is necessarily real, it is not equal to λ^2 , but it equals $|\lambda|^2 = \lambda\bar{\lambda}$. Relative prototile frequencies and areas can be calculated from the right and left PF eigenvectors as usual. Figure 1.11.3 shows a patch of the resulting tiling.

Remark 1.11.1. Due to the complicated path structure of the boundary, which produced the antennas that had to be removed in order to construct the fractally shaped prototiles, the corresponding analysis of the Hausdorff dimensions is considerably more involved than for a simple Koch-type curve. Bernd Sing has analysed this situation [47] and found the following results.

The Hausdorff dimension of the antennas is given by

$$\frac{\log(\kappa)}{\log(|\lambda|)} \approx 1.6355,$$

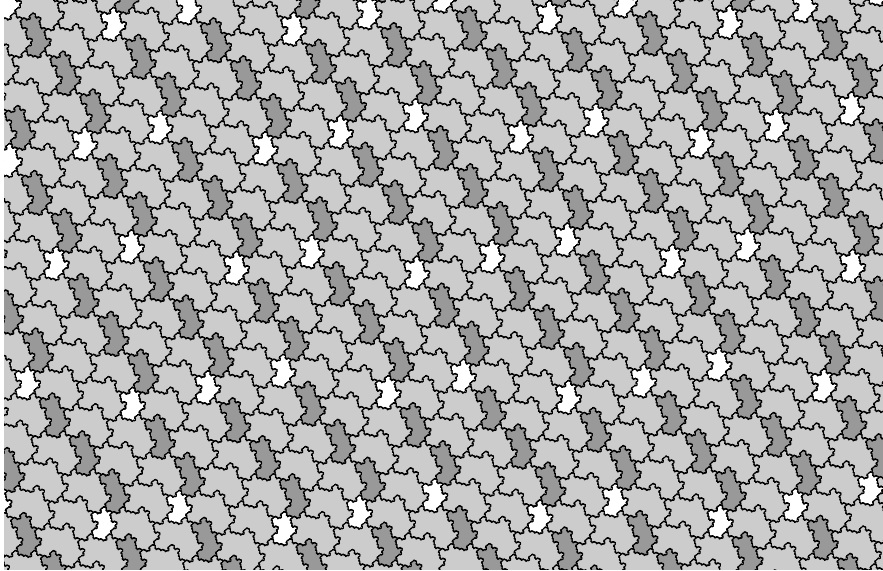


FIGURE 1.11.3. A patch of the fractal version of the inflation tilings.

where $\kappa \approx 2.1479$ is the unique real root of the polynomial $x^3 - x^2 - 2x - 1$. The Hausdorff dimension of the boundaries of the prototiles is considerably smaller. By the standard technique to derive an IFS for the boundary pieces (three are needed here), the Hausdorff dimension turns out to be

$$\frac{\log(\kappa')}{\log(|\lambda|)} \approx 1.1918,$$

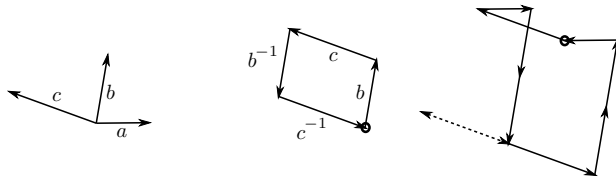
where $\kappa' \approx 1.7455$ is the unique positive real root of the quartic polynomial $x^4 - x^2 - 3x - 1$. \diamond

Several other inflation rules can be constructed in this way; browse, for instance, for those entries in [21] that are due to Harriss or Kenyon, or for entries with ‘dual’ in the title. One may use F_n for $n \geq 3$, yielding n line segments and $\binom{n}{2}$ prototiles. In all of these examples, the tiles usually occur in only one orientation in the tiling. Thus, the most prominent inflation rules (such as Penrose, Ammann–Beenker, chair, table and so on) do not arise from automorphisms of F_n in this way. Moreover, not every automorphism of F_n leads to an inflation. On the one hand, the automorphism may not yield an appropriate (complex) value for λ . On the other hand, the polygon given by the edge paths corresponding to $\sigma(T_i)$ is not necessarily tileable by the prototiles. For instance, the edge path might be self-intersecting. As an

example, consider the automorphism

$$\Phi(a) = b, \quad \Phi(b) = c, \quad \Phi(c) = ab^{-2}c.$$

This yields another complex inflation factor, namely $\lambda \approx 0.215 + 1.307i$. If we identify a with 1, b with λ and c with λ^2 as above, the prototile $bcb^{-1}c^{-1}$ and the edge path $cab^{-2}cc^{-1}c^{-1}b^2a^{-1}$ of its possible supertile look as follows,



It is not clear whether this technique can produce a proper inflation rule in this case. More generally, it would be nice to derive a criterion to decide which automorphisms of free groups give rise to inflation rules for tilings.

Remark 1.11.2. This construction also has a strong connection to model sets and cut-and-project schemes (CPS, see [AO1, Sec. 7.2]). In general, one may start this construction with an automorphism Φ of the free group with n generators for any $n \geq 3$. In the case of $n = 3$, if $\Phi^{-1}(a), \Phi^{-1}(b), \Phi^{-1}(c)$ contain only a, b, c (and not their inverses), the resulting tilings may be generated by a CPS. In particular, if $\Phi(a) = b$ and $\Phi(b) = c$, the PF eigenvector of the inflation matrix M_Φ has entries $(1, \lambda_{PF}, \lambda_{PF}^2)$. In this case, a standard construction applies: The fractal version of the two-dimensional tiling generated by Φ as described above is the dual tiling of the one-dimensional tiling generated by Φ^{-1} read backwards; compare [2, 23]. For more on this duality, see [AO1, Rem. 7.6] and references therein, or [17, 18]. \diamond

1.12. Mixed inflations

So far, we have encountered several generalisations of inflation rules, such as inflations with infinitely many prototiles or with overlapping tiles, or inflations with empty prototiles. Another generalisation consists of applying not one, but several different inflation rules $\sigma_1, \sigma_2, \dots, \sigma_n$. These inflations have to be chosen such that they are compatible. For simplicity, they should use the same inflation factor λ and the same prototiles T_1, \dots, T_m . This guarantees that the inflated prototiles λT_i can be dissected according to each of the inflations σ_i . The simplest example one may think of is described in [26]. Consider the two Fibonacci substitutions,

$$\varrho: \begin{array}{l} a \mapsto ab \\ b \mapsto a \end{array} \quad \text{and} \quad \varrho': \begin{array}{l} a \mapsto ba \\ b \mapsto a \end{array};$$

compare [AO1, Ex. 4.6 and Rem. 4.6]. The general idea of mixing these two substitutions can be realised in two different ways.

Firstly, one may apply one out of two substitutions σ_1, σ_2 to *all* tiles in each step: $\sigma_{i_1}(T_1), \sigma_{i_2}(\sigma_{i_1}(T_1))$, etc. If the sequence (i_j) is periodic, this yields nothing new. For example, if the sequence is $122\ 122\ 122\ 122\ \dots$, the resulting inflation is just $(\sigma_2)^2\sigma_1$. More generally, we may choose the i_j in a non-periodic manner, either deterministically (according to a Fibonacci sequence, say) or randomly in each step. In doing so, we leave the realm considered so far, and enter the regime of *S-adic* systems. We refer to [10, 9, 38, 39] for results on ergodicity and complexity of such mixed symbolic substitutions, and to [24] for some results on the cohomology of mixed substitutions.

As far as we know, there are few higher-dimensional examples of this type of construction in the literature; compare [25] and references therein (see also the references in Section 1.13). Note that, in the one-dimensional case, mixing the two Fibonacci substitutions ϱ and ϱ' in this way still generates nothing new, because they both define the same hull. A little later, we shall briefly discuss a two-dimensional example where this type of approach does yield something new.

Secondly, one may apply different substitutions on *individual* tiles randomly. This is briefly described for the two variants of the Fibonacci substitution in [AO1, Sec. 11.2.3]. A random application of ϱ and ϱ' means that one fixes $p \in (0, 1)$. Then, in each step of the substitution, a letter b is replaced by a , an a is replaced by ab with probability p , and by ba with probability $1 - p$. Such a can conveniently be represented as

$$b \mapsto a \mapsto \begin{cases} ab, & \text{with probability } p, \\ ba, & \text{with probability } 1 - p. \end{cases}$$

Considering the resulting sequences as tilings of the real line (with the usual interpretation of a as an interval of length $\tau = \frac{1}{2}(1 + \sqrt{5})$ and b as an interval of length 1) one may also ask for diffraction properties of the corresponding tilings. Recent results on the diffraction spectrum were obtained for the hull $\mathbb{X}_{\text{rand}(\varrho, \varrho')}$ of the random Fibonacci substitutions (and more generally, random noble mean substitutions) in [37, 51, 3]. In particular, it is shown that the diffraction spectrum of the random Fibonacci substitution contains no singular continuous part, which was left open in [26].

Theorem 1.12.1 ([37, 51, 3]). *The diffraction measure ω of $\mathbb{X}_{\text{rand}(\varrho, \varrho')}$, viewed as a dynamical system, satisfies*

$$\omega = \omega_{\text{pp}} + \omega_{\text{ac}},$$

where ω_{pp} is a non-trivial pure point measure and where ω_{ac} is a non-trivial

absolutely continuous measure. Simultaneously, this ω is also the diffraction measure of almost all individual elements of the hull. \square

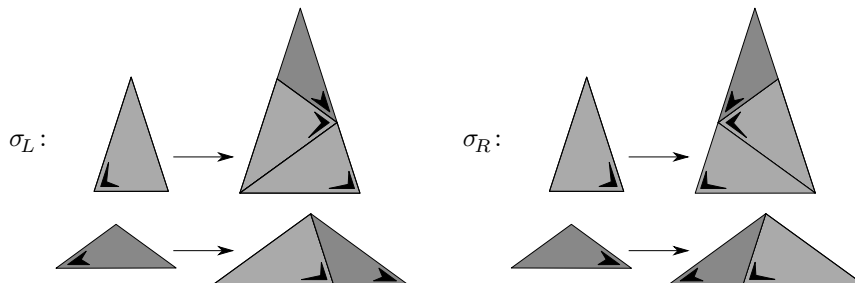
Moreover, exact formulas are given for the intensities of the pure point part of the diffraction spectrum and for the density of the absolutely continuous part. The latter is given in the form of a series that converges uniformly (to the Radon–Nikodym density). The ‘almost all’ in the theorem above is a consequence of the fact that the usual Fibonacci hull \mathbb{X}_ϱ is a (small) subset of $\mathbb{X}_{\text{rand}(\varrho, \varrho')}$. These and other exceptional elements, taken together, have zero measure in the stochastic hull.

Similar results hold for local mixtures of the two possible period doubling substitutions,

$$\begin{aligned} a &\mapsto \begin{cases} ab, & \text{with probability } p, \\ ba, & \text{with probability } 1 - p, \end{cases} \\ b &\mapsto aa. \end{aligned}$$

Interestingly, for $p = \frac{1}{2}$, the pure point part of the spectrum vanishes outside \mathbb{Z} , whereas it is dense on the real line for $p \neq \frac{1}{2}$; see [3].

Apart from [26], there is very little known about mixed, respectively random, inflations in more than one dimension. A two-dimensional example from [26] uses a chiral variant of the Penrose inflation rule for triangles,



Note that both inflation rules use only rotated and translated copies of the prototiles. Consequently, σ_R is the mirror image of σ_L , and the hulls \mathbb{X}_{σ_L} and \mathbb{X}_{σ_R} are mirror images of each other (and they are not equal, compare Figure 1.12.1). In contrast to the Fibonacci substitutions ϱ and ϱ' above, σ_L and σ_R define different hulls. Hence mixing them globally (that is, applying one of the two inflations to *all* tiles in each step) yields a much bigger hull $\mathbb{X}_{\text{mix}(\sigma_L, \sigma_R)}$, containing both \mathbb{X}_{σ_L} and \mathbb{X}_{σ_R} . Figure 1.12.2 shows a patch from a tiling in $\mathbb{X}_{\text{mix}(\sigma_L, \sigma_R)}$.

This approach has not yet been studied in detail (but compare Section 1.13). We refer to [25] for more inflations that can be mixed in this way, i.e., inflations with the same factor and the same prototiles. Mixing

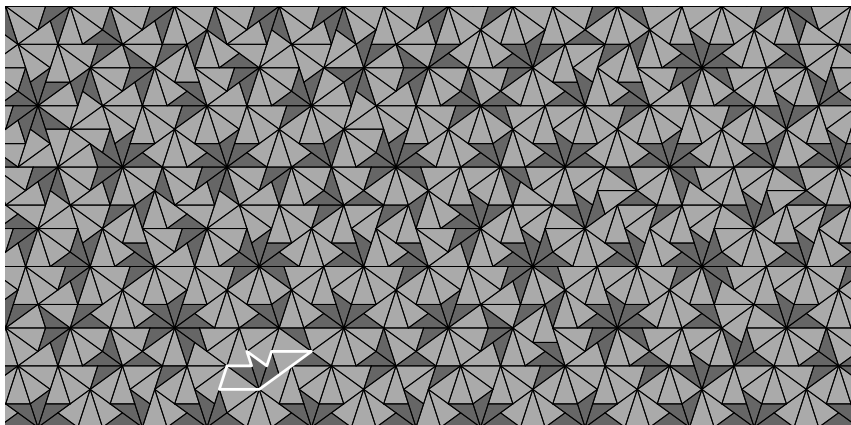


FIGURE 1.12.1. A patch of the left chiral Penrose tiling (in its version with golden triangles) generated by the inflation rule σ_L . Note the small patch consisting of three small triangles and two big triangles in the lower left part, indicated by a white contour. While the tiling contains rotated and translated copies of this patch, it does not contain any reflected copy.

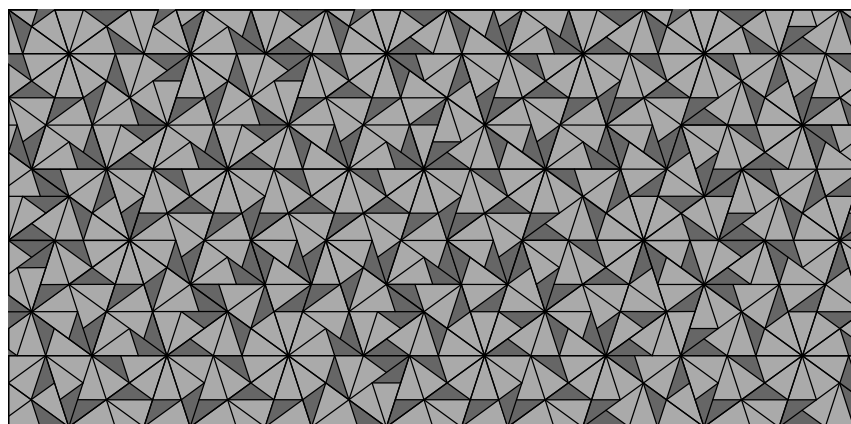


FIGURE 1.12.2. A patch of a mixed chiral Penrose tiling. More precisely, a patch from $(\sigma_2)^2(\sigma_1)^3(\sigma_2)^2(T)$, where T denotes the bigger triangle. Obviously, there are patches in this tiling that do not appear in the chiral Penrose tiling of Figure 1.12.1.

σ_1 and σ_2 locally (that is, applying to each tile σ_1 with probability p , and σ_2 with probability $1 - p$) yields an even larger hull $\mathbb{X}_{\text{rand}(\sigma_L, \sigma_R)}$, containing $\mathbb{X}_{\text{mix}(\sigma_L, \sigma_R)}$ (hence \mathbb{X}_{σ_L} and \mathbb{X}_{σ_R}) as subsets. First steps in investigating diffraction properties of the two-dimensional tilings that result from this approach are obtained in [26, 52].

1.13. Fusion tilings

In the previous section, the constructions used different inflations in each step. One may go even further than this. Probably the most general idea goes under the name of *fusion tilings*, which were introduced in [13].

A fusion tiling is generated by the following process. Consider a set of prototiles $\mathcal{P}_0 = \{P_0(1), P_0(2), \dots, P_0(m_0)\}$. Choose some finite collection of patches, $\mathcal{P}_1 = \{P_1(1), P_1(2), \dots, P_1(m_1)\}$, where each patch is built from prototiles in \mathcal{P}_0 . In the next step, choose some finite collection $\mathcal{P}_2 = \{P_2(1), P_2(2), \dots, P_2(m_2)\}$ of patches that are (measure-wise disjoint) unions of patches in \mathcal{P}_1 . Continue this process; that is, in step i , choose some finite collection of patches $\mathcal{P}_i = \{P_i(1), P_i(2), \dots, P_i(m_i)\}$ that are (measure-wise disjoint) unions of patches in \mathcal{P}_{i-1} . A tiling \mathcal{T} of \mathbb{R}^d is called a *fusion tiling* (with respect to the family $\{\mathcal{P}_i\}_i$) if any patch in \mathcal{T} is contained in some $P_i(k) \in \mathcal{P}_i$. The family $\{\mathcal{P}_i\}_i$ is called the *fusion rule*.

Note that the tiling space of a fusion rule can be empty, for instance if the inner radii of all patches in the fusion rule are bounded by some common constant. Obviously, all inflation tilings are fusion tilings: Just take the level- n supertiles as the patches in \mathcal{P}_n . Moreover, all FLC tilings are fusion tilings: Just define \mathcal{P}_i as the set of all connected patches in \mathcal{T} which contain i tiles or fewer. Consequently, it is plausible that this concept is far too general to prove any reasonable results on fusion tilings. Nevertheless, it is possible to define notions like primitivity or minimality for fusion tilings, and to obtain some general results on fusion tilings that are well-behaved, but still far away from being inflation tilings; see, for instance, [13] for some general results (such as Thms. 4.10, 4.13 and 5.3) and for several amazing examples. This new realm of fusion tilings is much too big to be explored more than superficially in this section.

Let us sketch some possibilities with the following example, which is a variant of [13, Ex. 3.7]. Let the prototiles be two unit squares, distinguished by colour — one black square and one white square, say. The fusion rule is indicated in Figure 1.13.1. It essentially consists of applying different inflation rules in each step. In the language of inflation rules, the level- $(k+1)$ supertile $P_{k+1}(1)$ consists of $2^k \times 2^k$ level- k supertiles $P_k(1)$, surrounded by a collar of $4 \cdot (2^k + 1)$ level- k supertiles $P_k(2)$. The level- $(k+1)$ supertile $P_{k+1}(2)$ is defined analogously, by just reversing the roles of $P_k(1)$ and $P_k(2)$. Hence, the *transition matrices*, which are the matrices counting the number of copies of $P_k(1)$ and of $P_k(2)$ in $P_{k+1}(i)$, are given by $A_k = \begin{pmatrix} 4^k & 4(2^k+1) \\ 4(2^k+1) & 4^k \end{pmatrix}$.

Figure 1.13.2 shows a patch of a resulting tiling. Note that it is generally unclear how to define a fixed point of a fusion rule. However, in this particular example, this is possible. Start with a (2×2) -patch of black squares $P_0(2)$,

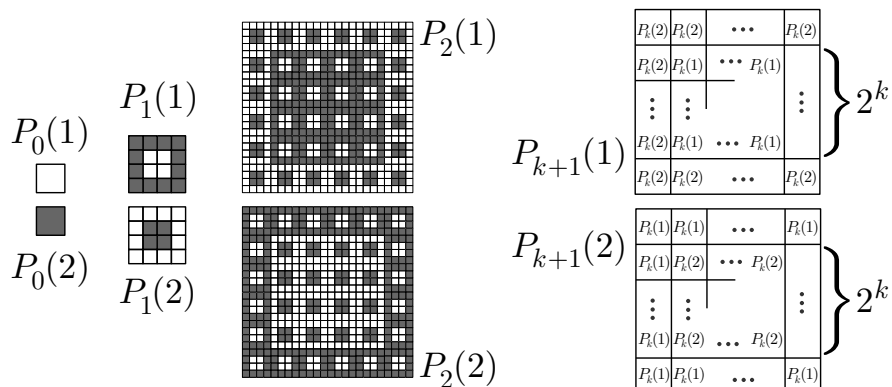


FIGURE 1.13.1. A fusion rule, given by using different inflation rules in each step. In particular, $P_{k+1}(1)$ consists of a $(2^k \times 2^k)$ -block of copies of $P_k(1)$ and a collar of copies of $P_k(2)$.

with the common vertex as the origin. The second iteration (four copies of $P_2(2)$ around the origin) contains the first patch in its centre. Inductively, four copies of $P_{2k+2}(2)$ contain a patch of four copies of $P_{2k}(2)$ in its centre. This sequence of patches converges to a tiling \mathcal{T} with respect to the local topology.

This example was chosen for the sake of visualisation. The relative and absolute frequencies of white and black squares are close to $\frac{1}{2}$. More precisely, they are given by the infinite product

$$\frac{1}{2} \pm \frac{1}{2} \prod_{k=1}^{\infty} \frac{2^{2k} - 4(2^k + 1)}{2^{2k} + 4(2^k + 1)} \approx \frac{1}{2} \pm 0.002704495,$$

if the seed consists of either black or white squares only, with the larger frequency for the tiles of the same colour as the seed. If one replaces the powers of 2 in the definition of the fusion rule above by powers of 10 (as is the case in [13, Ex. 3.7]), the frequencies become more unbalanced. Firstly, in the analogue \mathcal{T}' of the tiling \mathcal{T} constructed above (starting with four copies of black squares $P_0(2)$), black squares are even more frequent than white squares. Secondly, there is another tiling \mathcal{T}'' , constructed analogously by starting with four copies of white squares $P_0(1)$, in which white squares are much more frequent than black squares. Here, the frequencies are

$$\frac{1}{2} \pm \frac{1}{2} \prod_{k=1}^{\infty} \frac{10^{2k} - 4(10^k + 1)}{10^{2k} + 4(10^k + 1)} \approx \frac{1}{2} \pm 0.177754871.$$

Since both tilings, \mathcal{T}' and \mathcal{T}'' , contain supertiles of all levels, they are both contained in the hull of \mathcal{T}' . Consequently, the hull is not uniquely ergodic, because it supports at least two ergodic measures.

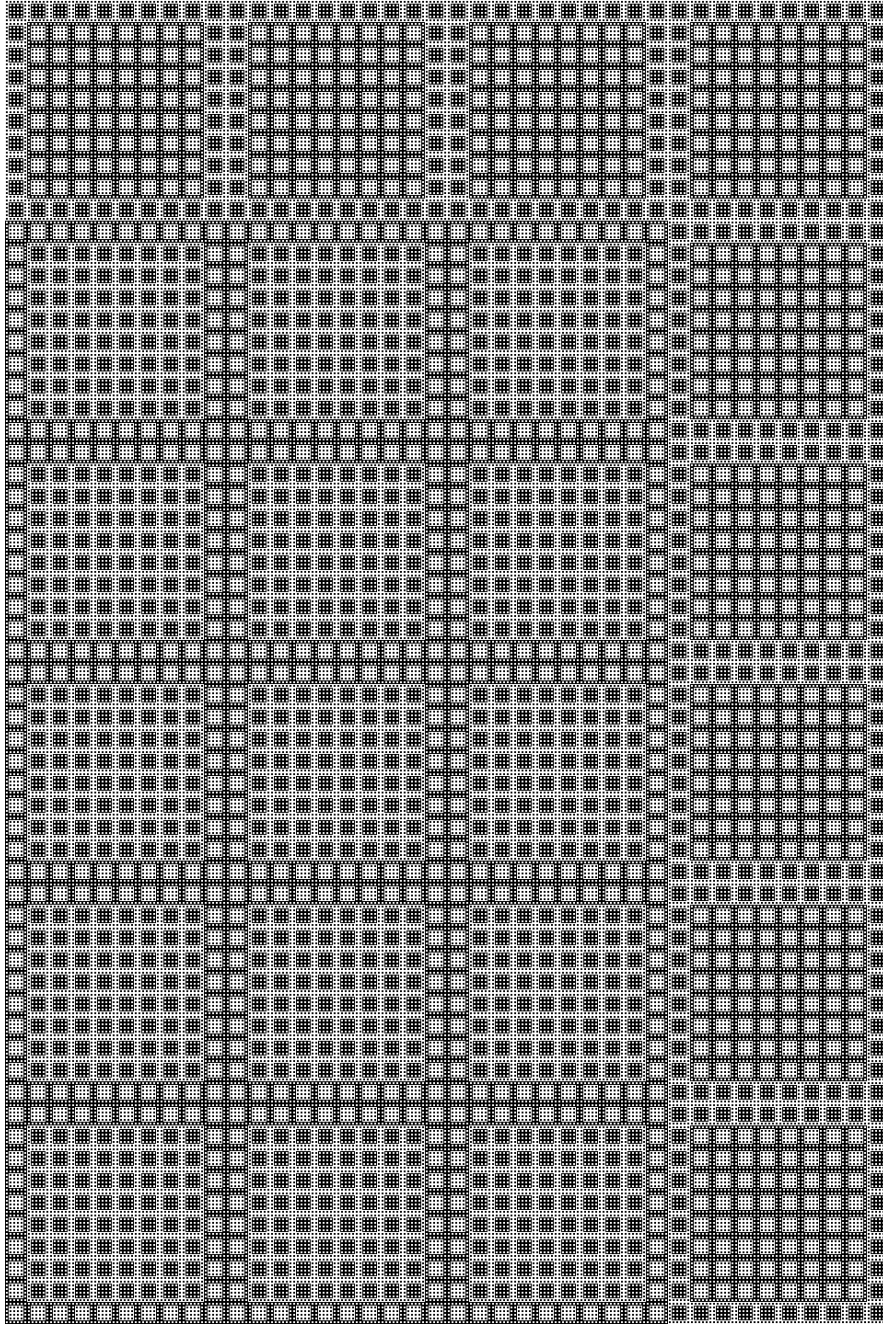


FIGURE 1.13.2. Part of the patch $P_4(1)$ of the fusion rule of Figure 1.13.1.

Several further interesting examples might arise from similar fusion rules. This huge field remains to be explored further.

Acknowledgements. It is a pleasure to thank everyone who has contributed to the Tilings Encyclopedia, in particular Jan Pieniak, Iwan Suschko, José Vizcaino, Kai Lüking and Tristan Storch. Special thanks to Michael Baake and Uwe Grimm for valuable help with content, images and formulations, and to Franz Gähler, Dan Rust and Bernd Sing for several helpful discussions, comments and additions.

References

- [AO1] Baake M. and Grimm U. (2013). *Aperiodic Order. Vol. 1: A Mathematical Invitation* (Cambridge University Press, Cambridge).
- [1] Aigner M. and Ziegler G.M. (2004). *Proofs from THE BOOK*, 5th ed. (Springer, Heidelberg).
- [2] Arnoux P., Harriss E.O., Ito S. and Furukado M. (2011). Algebraic numbers, group automorphisms and substitution rules on the plane, *Trans. Amer. Math. Soc.* **363**, 4651–4699.
- [3] Baake M., Spindeler T. and Strungaru N. (2017). Diffraction of compatible random substitutions in one dimension, in preparation.
- [4] Berthé V. and Siegel A. (2005). Tilings associated with beta-numeration and substitutions, *Integers* **5**, A2 (46 pages).
- [5] Cromwell P.R. (2009). The search for quasi-periodicity in Islamic 5-fold ornament, *Math. Intelligencer* **31**, 36–56.
- [6] Danzer L. (2001). An inflation-species of planar triangular tilings which is not repetitive, *Ferroelectrics* **250**, 163.
- [7] Danzer L. (2004). Inflation species of planar tilings which are not of locally finite complexity, *Proc. Steklov Inst. Math.* **239**, 108–116.
- [8] Danzer L., Grünbaum B. and Klee V. (1982). Can all tiles of a tiling have five-fold symmetry? *Amer. Math. Monthly* **89**, 568–570 and 583–585.
- [9] Durand F. (2000). Linearly recurrent subshifts have a finite number of non-periodic subshift factors, *Ergodic Th. & Dynam. Syst.* **20**, 1061–1078. [arXiv:0807.4430](#).
- [10] Ferenczi S. (1996). Rank and symbolic complexity, *Ergodic Th. & Dynam. Syst.* **16**, 663–682.
- [11] Frank N.P. (2008). A primer of substitution tilings of the Euclidean plane, *Expos. Math.* **26**, 295–326. [arXiv:0705.1142](#).
- [12] Frank N. (2015). Tilings with infinite local complexity. In *Mathematics of Aperiodic Order*, Kellendonk J., Lenz D. and Savinien J. (eds.), pp. 223–257 (Birkhäuser, Basel). [arXiv:1312.4987](#).
- [13] Frank N. and Sadun L. (2014). Fusion: A general framework for hierarchical tilings of \mathbb{R}^d , *Geom. Dedicata* **171**, 149–186. [arXiv:1101.4930](#).
- [14] Frank N. and Robinson E.A. (2008). Generalized β -expansions, substitution tilings, and local finiteness, *Trans. Amer. Math. Soc.* **360**, 1163–1177. [arXiv:math.DS/0506098](#).

- [15] Frettlöh D. (1998). *Inflationäre Pflasterungen der Ebene mit minimaler Musterfamilie und D_{2m+1} -Symmetrie*, Diploma thesis (Dortmund University).
- [16] Frettlöh D. (2002). *Nichtperiodische Pflasterungen mit ganzzahligem Inflationsfaktor*, Ph.D. thesis (Dortmund University), available at <https://hdl.handle.net/2003/2309>.
- [17] Frettlöh D. (2005). Duality of model sets generated by substitutions, *Rev. Roumaine Math. Pures Appl.* **50**, 619–639. [arXiv:math/0601064](https://arxiv.org/abs/math/0601064).
- [18] Frettlöh D. (2008). Self-dual tilings with respect to star-duality, *Theoret. Comput. Sci.* **391**, 39–50. [arXiv:0704.2528](https://arxiv.org/abs/0704.2528).
- [19] Frettlöh D. (2008). Substitution tilings with statistical circular symmetry, *European J. Combin.* **29**, 1881–1893. [arXiv:0803.2172](https://arxiv.org/abs/0803.2172).
- [20] Frettlöh D. (2008). About substitution tilings with statistical circular symmetry, *Philos. Mag.* **88**, 2033–2039. [arXiv:0704.2521](https://arxiv.org/abs/0704.2521).
- [21] Frettlöh D., Gähler F. and Harriss E. *Tilings Encyclopedia*, available at <https://tilings.math.uni-bielefeld.de>.
- [22] Frettlöh D. and Hofstetter K. (2015). Inductive rotation tilings, *Proc. Steklov Inst. Math.* **288**, 269–280. [arXiv:1410.0592](https://arxiv.org/abs/1410.0592).
- [23] Gähler F. (2010). MLD relations of Pisot substitution tilings, *J. Phys.: Conf. Ser.* **226**, 012020: 1–6. [arXiv:1001.2744](https://arxiv.org/abs/1001.2744).
- [24] Gähler F. and Maloney G.R. (2013). Cohomology of one-dimensional mixed substitution tiling spaces, *Topol. Appl.* **160**, 703–719. [arXiv:1112.1475](https://arxiv.org/abs/1112.1475).
- [25] Gähler F., Kwan E.E. and Maloney G.R. (2015). A computer search for planar substitution tilings with n -fold rotational symmetry, *Discr. Comput. Geom.* **53**, 445–465. [arXiv:1404.5193](https://arxiv.org/abs/1404.5193).
- [26] Godrèche C. and Luck J.M. (1989). Quasiperiodicity and randomness in tilings of the plane, *J. Stat. Phys.* **55**, 1–28.
- [27] Goodman-Strauss C. (1996). A non-periodic self-similar tiling with non-unique decomposition, Technical Report UofA-R-126 (University of Arkansas).
- [28] Goodman-Strauss C. (1998). Matching rules and substitution tilings, *Ann. of Math.* **147**, 181–223.
- [29] Gummelt P. (2006). *Private communication*.
- [30] Harriss E.O. (2005). Non-periodic rhomb substitution tilings that admit order n rotational symmetry, *Discr. Comput. Geom.* **34**, 523–536.
- [31] Kannan S. and Soroker D. (1992). Tiling polygons with parallelograms, *Discr. Comput. Geom.* **7**, 175–188.
- [32] Kari J. and Rissanen M. (2016). Sub Rosa, a system of quasiperiodic rhombic substitution tilings with n -fold rotational symmetry, *Discr. Comput. Geom.* **55**, 972–996. [arXiv:1512.01402](https://arxiv.org/abs/1512.01402).
- [33] Kenyon R. (1992). Self-replicating tilings. In *Symbolic Dynamics and its Applications*, Walters P. (ed.), CONM 135, pp. 239–263 (AMS, Providence, RI).
- [34] Kenyon R. (1993). Tiling a polygon with parallelograms, *Algorithmica* **9**, 382–397.
- [35] Kenyon R. (1996). The construction of self-similar tilings, *Geom. Funct. Anal. (GAFA)* **6**, 417–488. [arXiv:math.MG/9505210](https://arxiv.org/abs/math.MG/9505210).
- [36] Maloney G.R. (2015). On substitution tilings of the plane with n -fold rotational symmetry, *Discr. Math. Theor. Comput. Sci.* **17**, 395–412. [arXiv:1409.1828](https://arxiv.org/abs/1409.1828).

- [37] Moll M. (2014). Diffraction of random noble means words, *J. Stat. Phys.* **156**, 1221–1236. [arXiv:1404.7411](#).
- [38] Nilsson J. (2012). On the entropy of a family of random substitutions, *Monatsh. Math.* **168**, 563–577. [arXiv:1103.4777](#).
- [39] Nilsson J. (2013). On the entropy of a two step random Fibonacci substitution, *Entropy* **15**, 3312–3324. [arXiv:1303.2526](#).
- [40] Pautze S. (2017). Cyclotomic aperiodic substitution tilings, *Symmetry* **9**, 19: 1–41. [arXiv:1606.06858](#).
- [41] Radin C. (1997). Aperiodic tilings, ergodic theory, and rotations. In *The Mathematics of Long-Range Aperiodic Order*, NATO ASI Series C 489, Moody R.V. (ed.), pp. 403–441 (Kluwer, Dordrecht).
- [42] Robinson E.A. (1999). On the table and the chair, *Indag. Math.* **10**, 581–599.
- [43] Sadun L. (1998). Some generalizations of the pinwheel tiling, *Discr. Comput. Geom.* **20**, 79–110. [arXiv:math.GR/9712263](#).
- [44] Sadun L. (2008). *Private communication*.
- [45] Senechal M. (2004). The mysterious Mr. Ammann, *Math. Intelligencer* **26**, 10–21.
- [46] Sing B. (2006). *Pisot Substitutions and Beyond*, PhD thesis (Univ. Bielefeld).
- [47] Sing B. (2016). *Private communication*.
- [48] Sloane N.J.A. (ed.). *The On-Line Encyclopedia of Integer Sequences*, available at <https://oeis.org/>.
- [49] Socolar J.E.S. and Taylor J.M. (2011). An aperiodic hexagonal tile, *J. Combin. Theory A* **118**, 2207–2231. [arXiv:1003.4279](#).
- [50] Solomyak B. (1998). Non-periodicity implies unique composition property for self-similar translationally finite tilings, *Discr. Comput. Geom.* **20**, 265–279.
- [51] Spindeler T. (2017). Diffraction intensities of a class of binary Pisot substitutions via exponential sums, *Monatsh. Math.* **182**, 143–153. [arXiv:1608.01969](#).
- [52] Spindeler T. (2018). *On the Spectral Theory of Random Inflation Systems*, PhD thesis (Bielefeld University, in preparation).
- [53] Thurston W. (1989). Groups, tilings and finite state automata, unpublished lecture notes, available at <http://timo.jolivet.free.fr/docs/ThurstonLectNotes.pdf>.
- [54] Washington L.C. (1997). *Introduction to Cyclotomic Fields*, 2nd ed. (Springer, New York).